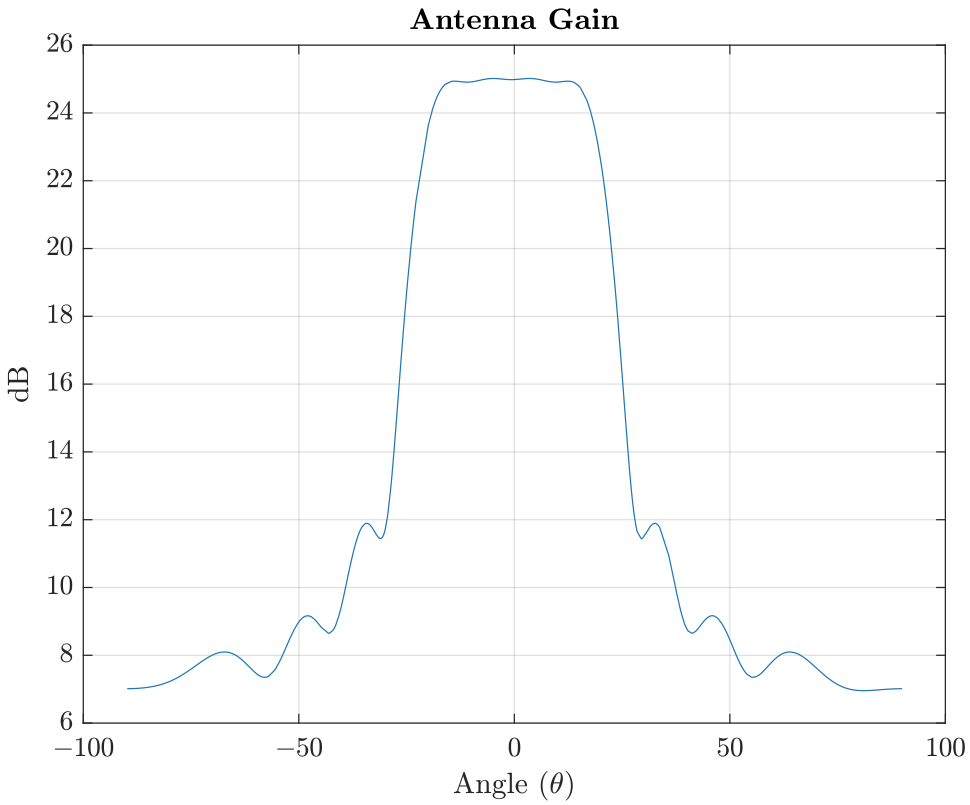


# MIMO-waveforms for GMTI radar

## A study on the use of MIMO waveforms to decrease MDV in GMTI radar

Master's thesis in Engineering Mathematics and Computational Science

MAX JISONSUND

DEPARTMENT OF ELECTRICAL ENGINEERING

CHALMERS UNIVERSITY OF TECHNOLOGY
Gothenburg, Sweden 2024
www.chalmers.se

Master's thesis 2024

# MIMO-waveforms for GMTI radar

A study on the use of MIMO waveforms to decrease MDV in GMTI radar

MAX JISONSUND


CHALMERS
UNIVERSITY OF TECHNOLOGY

Department of Electrical Engineering
Chalmers University of Technology
Gothenburg, Sweden 2024

MIMO-waveforms for GMTI radar
A study on the use of MIMO waveforms to decrease MDV in GMTI radar
MAX JISONSUND

© MAX JISONSUND, 2024.

Supervisors: Patrik Dammert (SAAB AB), Tomas McKelvey (Chalmers University of Technology)
Examiner: Tomas McKelvey, Department of Electrical Engineering

Master's Thesis 2024
Department of Electrical Engineering
Chalmers University of Technology
SE-412 96 Gothenburg
Telephone +46 705880845

Cover: Antenna gain visualisation made with Matlab.

Typeset in LaTeX
Gothenburg, Sweden 2024

MIMO waveforms for GMTI radar
A study on the use of MIMO waveforms to decrease MDV in GMTI radar
Max Jisonsund
Department of Electrical Engineering
Chalmers University of Technology

# Abstract

This study investigates the use of MIMO waveforms in mitigating the effects of clutter in GMTI radar systems. Clutter, which is any unwanted reflection from the ground with a Doppler shift will affect the performance of a radar. In particular the minimum detectable velocity will increase. By applying MIMO waveforms it is possible to, in some cases, increase performance and decrease the minimum detectable velocity. This study has through simulations explored MIMO systems and compared these to traditional SIMO systems. Furthermore sparse arrays has also been explored and once again compared between MIMO and SIMO. Moreover this study has developed a unified model capable of simulating systems using for example SIMO, MIMO or sparse arrays. This serves as a valuable tool to perform further studies on the topic.

Keywords: Radar, Signal Processing, MIMO waveform, AESA.

# Acknowledgements

I would like to express my deepest gratitude to my supervisors Dr. Patrik Dammert and Professor Tomas McKelvey for their patience and help throughout this journey. Many thanks should also go to Dr. Stefan Eilertsen for our many discussions. Additionally, thanks to both Saab, Dr. Johan Backlund in particular, and Chalmers for giving me this opportunity.

I am also thankful for my colleagues at Saab for sharing their knowledge and expertise. Lastly, I am extremely grateful for my family, friends and partner. Their belief in me has kept my spirits high.

Max Jisonsund, Gothenburg, May 2024

# List of Acronyms

Below is the list of acronyms that have been used throughout this thesis listed in alphabetical order:

| | |
|---|---|
| MIMO | Multiple-Input, Multiple-Output |
| GMTI | Ground moving target indication |
| STAP | Space-time adaptive processing |
| SIMO | Single-input, Multiple-output |
| MDV | Minimum detectable velocity |
| SNR | Signal-to-noise ratio |
| SINR | Signal-to-interference and noise ratio |
| CP | Clutter-and-noise power |
| TX | Transmitter |
| RX | Receiver |
| PRF | Pulse repetition frequency |
| PRI | Pulse repetition interval |
| CPI | Coherent processing interval |
| FIR | Finite Impulse Response |
| RCS | Radar cross section |

# Nomenclature

Below various nomenclature is presented.

## Variables

| | |
|---|---|
| $N_k$ | Number of antenna elements |
| $N_p$ | Number of pulses in a CPI (Coherent processing interval) |
| $N_s$ | Number of point scatterers |
| $N_r$ | Number of fast-time samples |
| $F_n$ | Noise figure |
| $P_t$ | Peak transmitting power |
| $G_t$ | Transmitting gain |
| $\sigma$ | Radar cross section |
| $B$ | Bandwidth |
| $f_u$ | Spatial frequency |
| $f_d$ | Doppler frequency |

# Contents

# List of Figures

# List of Tables

# 1
# Introduction

Today radars form an integral part of our society with applications in weather monitoring, self-driving cars or even fall detection [1]–[3]. Apart from this radars are also used in the military, where they are used for a wide range of tasks from navigation to air surveillance [4]. This study will investigate the possibilities of using radar techniques to improve detection of moving objects. In particular one such technique, MIMO (multiple-input multiple-output), will be considered. MIMO has had great success in a wide range of fields, most notably in wireless communication but also in radars used for remote sensing [5]. This chapter will introduce the problem by first presenting some necessary background, then specify the purpose of this study and lastly present the limitations of the study.

## 1.1 Background

Ground moving target indication radar (henceforth GMTI) is a special case of the more general moving target indication (MTI), which is specifically designed for airborne platforms. It is based on a pulse-Doppler radar and its primary function is to detect moving objects on the ground [6]. This technique is built on the theory of space-time adaptive processing (STAP) or more generally space-time processing (STP) [7]. STP is an algorithm which was developed to handle different interferences that a radar is exposed to, such as clutter or jamming [8].

When a pulse-Doppler radar, mounted on an airborne platform, scans a volume for objects the electromagnetic waves will bounce off every object present. Since the platform is moving, waves reflected from the ground will present Doppler shifts of varying degree depending on the angle. This, together with any energy reflected from the ground, leads to what is called ground clutter [9]. Because of this, objects with velocities similar to that of the ground i.e., objects with low velocities or stationary objects will be difficult to detect.

To mitigate the effect of clutter one possible approach is to use MIMO in order to improve space-time processing, which in literature has been shown to increase performance in settings with clutter present [10]. In contrast to traditional GMTI systems, this technology is characterised by the fact that each antenna element transmits a unique waveform and that every channel is sampled in the receiver [11]. This is different compared to a traditional GMTI which only sends out scaled versions of the same waveform from each antenna element [9], [12].

## 1.2 Purpose

The purpose of this thesis is to examine the possibilities of increasing detection performance using MIMO waveforms in a GMTI radar system. This is to be performed by simulating an electronically scanned multichannel array. One way to measure such an improvement is to calculate the *minimum detectable velocity* (MDV) which describes the velocity of the slowest moving detectable object. Another possible way of evaluating the performance of such a radar is to, by ocular inspection, make a qualitative analysis of the performance. This analysis is to be done by comparing the MIMO case to a baseline case using SIMO (single-input, multiple-output).

## 1.3 Method

The principal method used in this study has been simulations using synthetic data. Radar setups used include, but is not limited t, small arrays, large arrays and sparse arrays. Furthermore waveforms has been varied between SIMO and MIMO with different types of MIMO waveforms. Regarding evaluation of results MDV has been the main quantitative metric which has been supplemented with qualitative arguments by ocular inspection of figures showing ratios such as signal-to-interference plus noise ratio or clutter-and-noise power.

## 1.4 Limitations

Only basic uniform linear array antennas will be modelled. This study is constrained to two cases; one with a larger uniform linear array of 24 antenna elements and one smaller array with 4 antenna elements. Even though the radar platform is assumed to be airborne all simulations will be limited to two dimensions. Furthermore the radar is, in the case with SIMO waveforms, only transmitting broadside i.e., in a direction orthogonal to the travel direction of the radar platform. On the receiving side the radar receives signals from all directions, both with SIMO and MIMO waveforms.

## 1.5 Reading Instructions

This report is built up of different chapters which have been split into different sections and subsections. For readers with lack of previous experience with radar it is suggested to read through chapter 2 in order to pick up the necessary understanding to comprehend the rest of the report. Chapter 2 starts off with a section on basic signal detection which is the base for this study, it then continuous with basics of radar theory before moving onto the signal processing chapter. These chapter together with chapter 4 is supposed to be clear enough so that someone with adequate

knowledge can reproduce the results. As soon as methods have been presented results follow in the subsequent chapter. Lastly a discussion of the results is presented together with conclusions and possible future work.

# 2
# Radar Theory

In the following sections basic radar theory will be presented. To begin with, the signal detection problem is presented which is the basis for this study. The aim of this chapter is to provide the theoretical framework needed to understand the results from this study.

## 2.1 Signal Detection

Detection is a way of extracting information from signals. To give this some context: Imagine an active radar, meaning one that emits radio waves and then receives the reflections. For this radar to be useful one needs to extract information from the received electromagnetic waves. If the emitted waves were to be reflected back without being affected the problem would be trivial. However, anything that interacts with the signal will affect it. This interference can be put into three categories: thermal noise, clutter and jamming [13]. This study has investigated thermal noise and clutter, meaning jamming has been ignored. Therefore the fundamental detection problem can be formulated as the binary hypothesis test

$$\begin{cases} H_0: & \mathbf{z} = \mathbf{c} + \mathbf{n} \\ H_1: & \mathbf{z} = \alpha\mathbf{s} + \mathbf{c} + \mathbf{n}, \end{cases} \tag{2.1}$$

where $H_0$ is the null hypothesis, $\mathbf{z}$ denotes the received signal, $\mathbf{c}$ denotes clutter, $\mathbf{n}$ denotes thermal noise, $\alpha$ is a constant and $\mathbf{s}$ denotes the sought-after signal [14]. All of the above variables are vectors except for $\alpha$ which is a scalar.

## 2.2 Introduction to Radar

There are numerous different types of radars available with one of the first documented usages of a radar was done by Christian Hülsmeyer in 1904 when he made a demonstration in Cologne, Germany. It was done by pointing a transmitter towards a river and when ships were hit the waves would reflect back to a receiver and the device, known as the Telemobiloskop, would be able to show the direction of the ship [15]. Today this version of a radar is accompanied by several other possible setups such as a monostatic radar which is a radar where both transmitter and receiver are mounted on the same platform. Every such antenna is built up of what is called antenna elements which either receives signals or transmits them. In one of the most trivial radars all signals received from respective antenna element is summed up and

then signal processing techniques are applied to this sum. However, given enough computing power it is also possible to collect data from all channels and process these vector valued signals. This is what is called a multichannel radar.

In figure 3.3 a multichannel radar containing $N_k$ antenna elements is pictured. It is an electronically scanned array which is a radar that electronically shifts the phase of every antenna element and it thereby can both transmit and receive in different directions. By assuming that the incoming wave is a plane wave such as the one in figure 3.3 the angle can be calculated by using the phase shift between antenna elements. This phase shift arises due to the fact that the minimum distance from a given wave to the first antenna is different from the minimum distance to the last antenna, given that a phase shift is presented otherwise the distances are all the same and the angle of arrival is zero. This plane wave approximation is valid if the source is in the far-field which is characterised by the distance $2D^2/\lambda$, where $D$ is the width of the aperture and $\lambda$ is the wavelength [14]. Furthermore it is possible to, by analysing different pulses, calculate the Doppler frequency and therefore also find the radial velocity of the target [16].

### 2.2.1 Radar Configurations and Waveforms

A radar system usually contains transmitters (TX) and receivers (RX) which can either be located close together or far apart. Furthermore it is also possible to use multiple spaced transmitters and receivers to build what is known as a multistatic radar. There are several reasons for choosing either one of the above configurations. However, one important thought to keep in mind when evaluating the possibilities is the physical limitations that are present.

The transmitters are able to generate electromagnetic waves of very high power (hundreds of kilowatts) while the receivers are very sensitive and are able to detect powers as low as picowatts. The implication of this is that if transmitters and receivers, which are close together, are activated at the same time self-jamming will be introduced which could also greatly harm the radar due to the high sensitivity in the receivers and the high power in the transmitters [14]. Another way to put this is that the transmitter will overload the receivers.

One of, if not the most important fundamentals of radar, is that they send out waveforms. Each waveform is characterised by its *frequency*, *amplitude* and *phase*. Given these attributes it is possible to describe any wave. Any electrical signal contains information and encoding this information is done by modulating either frequency, amplitude, phase or any combination of the three as a function of time. This function can be denoted as $m(t)$ and will be used in each following example of modulations. These differently modulated signals can be represented by $s(t)$ where a frequency modulated signal is given by

$$s(t) = A\cos\left(2\pi f_c t + r\int_0^t m(s)\mathrm{d}s\right), \tag{2.2}$$

in which $A$ is a constant, $f_c$ is the frequency of the carrier wave, $r$ is called the modulation index and $m(s)$ is the encoded information [17]. Furthermore the equations

$$s(t) = Am(t)\sin(2\pi f_c t), \tag{2.3}$$
$$s(t) = A\sin(2\pi f_c t + \beta m(t)), \tag{2.4}$$

represent an amplitude modulated signal and a phase modulated signal of the same signal model, respectively, where $\beta$ is a constant [17].

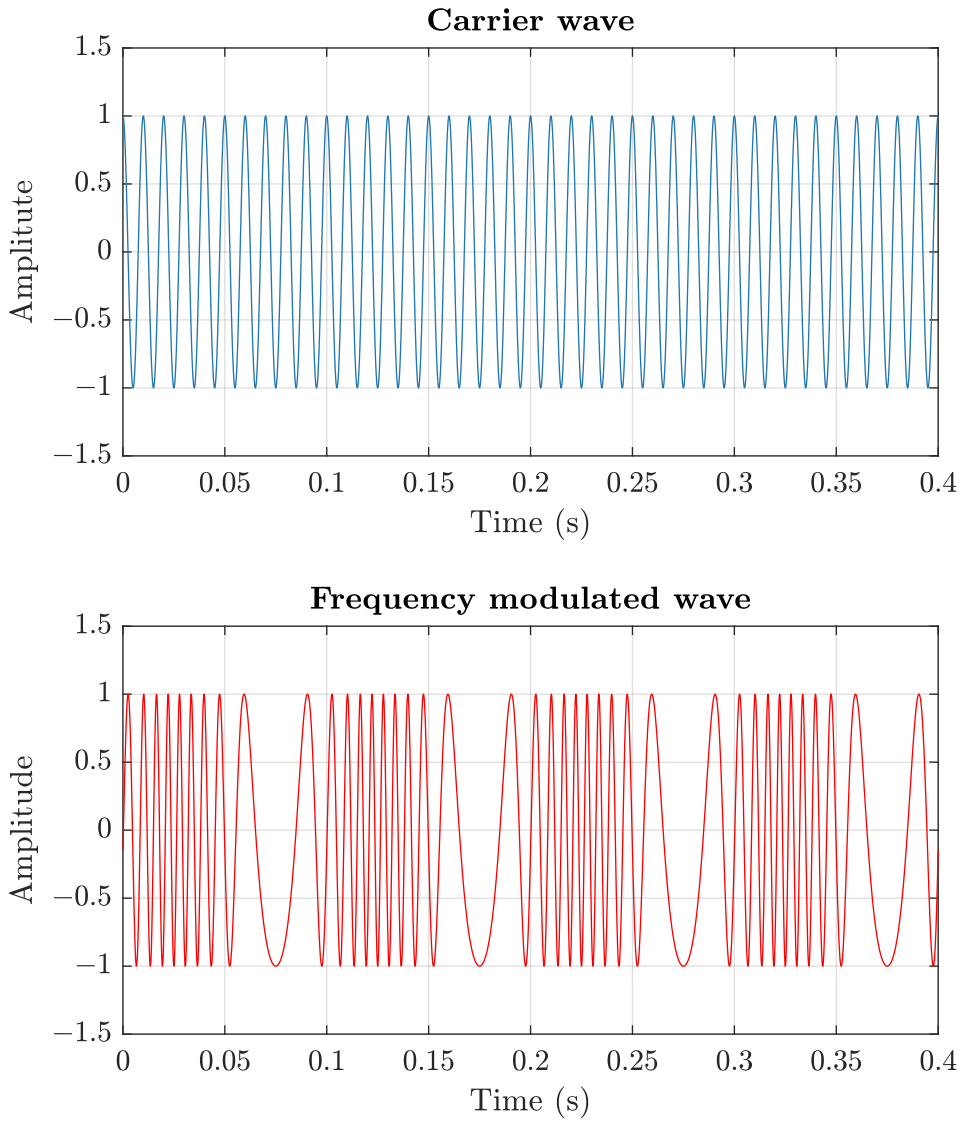


**Figure 2.1:** A visualisation of frequency modulation. The top figure shows the carrier wave. In the bottom figure an example of a frequency modulated wave is shown.

An example of a frequency modulated wave is shown in figure 2.1. Worth to note

is that this is a simple version of frequency modulation and that there are more complex methods available.

Moreover a radar transmitter can transmit continuous or pulsed waveforms. A continuous wave is a wave which is generated by having the transmitter transmit continually, while a pulsed waveform is characterised by transmitting the signal during a short duration of time. In figure 2.2 the pulsed waveform situation is illustrated. Every pulse has a width which is called the pulse width, $\tau$, and the frequency of pulses is specified by the pulse repetition frequency (PRF), which is the reciprocal of the pulse repetition interval (PRI). On the receiving end there is a delay ($\Delta t$) between the time when the pulse has been transmitted and when it is received. The delay between a received and a transmitted pulse can be used in order to find the range of the object by using

$$R = \frac{c\Delta t}{2}. \tag{2.5}$$

Notice also that there is a delay between transmitting and sampling which is to avoid self-jamming (2.5) [14]. With this logic every sample in *fast-time* will correspond to a single range interval. This means that fast-time is the time during sampling of a single pulse and *slow-time* on the other hand corresponds to different pulses. There is a delay between end of transmitting and beginning of sampling (receiving) which is inserted in order to avoid risk of self-jamming and harming the equipment. The interval in which electromagnetic waves are collected is called coherent processing interval (CPI). When receivers are active sampling frequency must be high enough in order not to miss any information. What is meant by this is that the time between samples must not be greater than the pulse width [14].

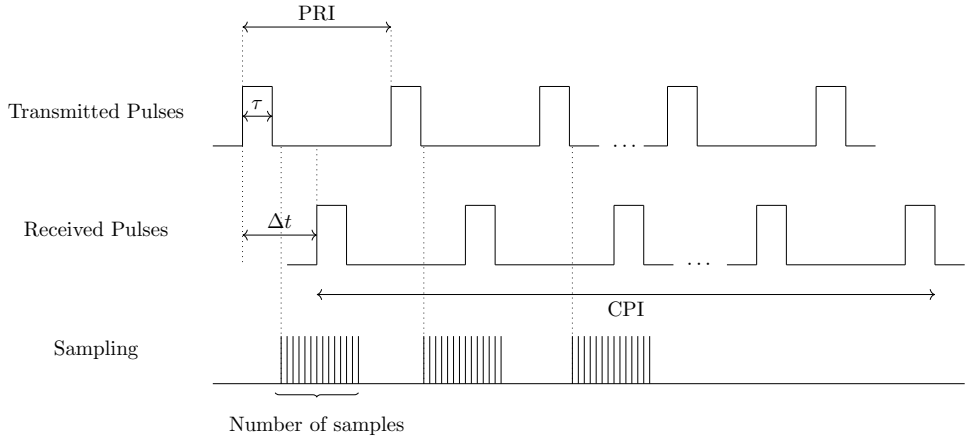


**Figure 2.2:** This figure illustrates a pulsed radar waveform. In the top, transmitted pulses with a pulse width of $\tau$ and a pulse repetition interval, PRI, is shown. In the middle, one can see the received pulses. There is a delay, $\Delta t$, between the transmitted and the received pulse which is used for finding the objects range. The time during which the received pulses are collected is called coherent pulse interval.

It is possible to store the received data in several different ways; however, one self-explanatory way of doing this is to use a data cube such as in figure 2.3. In this

figure every range bin is visaulised as a single matrix with dimensions $N_p \times N_k$, where $N_p$ is the number of pulses in one coherent pulse interval (CPI) and $N_k$ denotes the number of antenna elements.

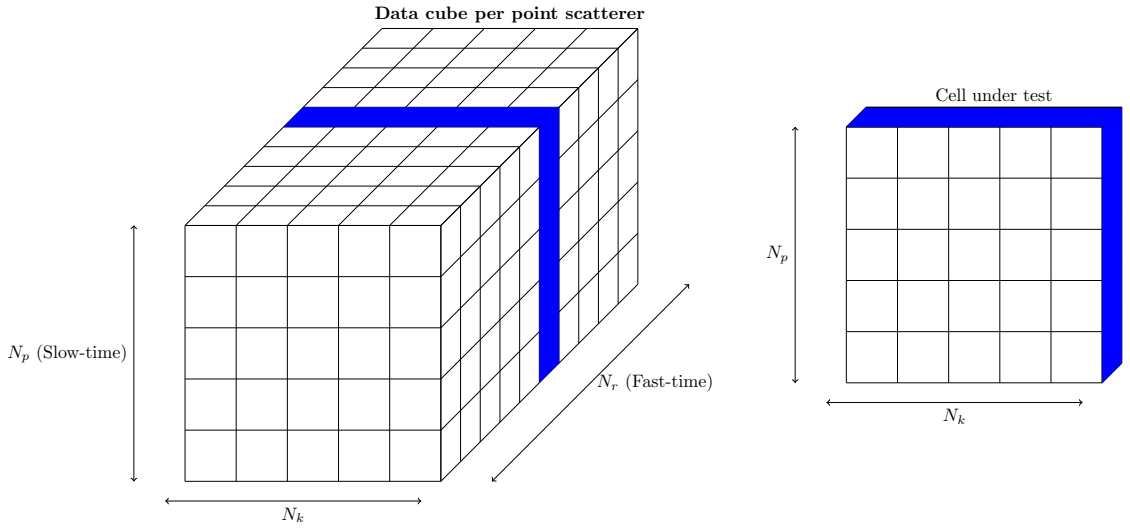


**Figure 2.3:** Data cube containing the collected data per every point scatterer. $N_k$ is given by the number of antenna elements, $N_p$ is given by the number of pulses received and $N_r$ is the number of fast-time samples.

In this study the data will not be organised in this way but it is still worth to note that this is the general way of doing it when working with experimental radar data.

### 2.2.2 The Radar Equation

The radar equation is most commonly used to estimate maximum detection range but it can also be used to examine performance of a radar by calculating a collection of ratios such as *signal-to-noise ratio* (SNR), *signal-to-interference plus noise ratio* (SINR) or *signal-to-clutter ratio* (SCR). The radar range equation can be written as

$$P_r = \frac{P_t G_t G_r \lambda^2 \sigma_0}{(4\pi)^3 R^4}, \tag{2.6}$$

where $P_t$ is the peak power of the transmitter, $G_t$ is the gain of the transmitter and $R$ is the distance to the reflecting object, $G_r$ is the gain of the receiver, $\lambda$ is the wavelength and $\sigma_0$ is the radar cross section. The peak power $P_r$ decreases with $R^4$ since EM waves have to travel both to the object and back, in other words the strength of the received radiation is inversely proportional to $R^4$. This corresponds to the signal power received by the radar. However, the radar also receives thermal noise given by

$$P_n = kT_0F_sB, \tag{2.7}$$

where $k$ is Boltzmann's constant, $T_0$ is the standard temperature, $F_s$ is the noise figure and $B$ denotes the receiver bandwidth [14]. By dividing the received power with the thermal noise power SNR is obtained as

$$\text{SNR} = \frac{P_t G_t G_r \lambda^2 \sigma}{(4\pi)^3 R^4 B k T_0 F_s}. \tag{2.8}$$

### 2.2.3 Radar Resolution

Resolution is a measure of how accurately a radar can differentiate between closely spaced objects. In this setting close does not simply mean objects close together in angle but also objects with similar Doppler frequency or range.

*Resolution in Angle*
Resolution in angle will depend on the main beam width in the antenna diagram. A typical antenna diagram takes the form of a sinc function where the main beam is the "beam" with the maximum amplitude. It is easy to realise that the width of this beam decides the angular resolution [14].

*Resolution in Doppler*
Regarding resolution in Doppler frequency one of the most important features, given a constant PRF, is the dwell time (CPI), or in other words the time during which the radar is looking at a certain target. During this time a number of pulses will be emitted and received by the radar. Depending on how many pulses, given a constant PRF, that are emitted the Doppler resolution will change. More specifically an increased number of pulses implies better resolution.

*Resolution in Range*
Range resolution of a radar is, when utilizing a pulse-Doppler radar, mainly dependent on the pulse width if pulse compression is not used. Theoretically a radar will be able to detect objects spaced by the distance the wave travels during half a pulse width. This means that the lowest spaced distance is given by

$$d_r \geq \frac{c\tau}{2} \tag{2.9}$$

where $c$ denotes speed of light and $\tau$ is the pulse width [14]. However, if pulse compression is implemented, which it in this study is, bandwidth is instead most important for range resolution. This is usually computed as

$$d_r = \frac{c}{2B}, \tag{2.10}$$

where $B$ is the bandwidth [14].

### 2.2.4 Radar ambiguities

Another important subject in radar theory is ambiguities. There will on one hand, in theory, always exist ambiguities both in velocity and in range. In practice on the other hand ambiguities will be dependent on PRF since given a small enough PRF

transmitted waves will have passed the horizon before the next pulse is transmitted. However, since this study has examined medium PRF systems it is still a very important subject. To manage this there are several possible approaches, some of which will be explained later on.

*Range Ambiguities*
Imagine that a pulse, call it $P1$, is sent out from the radar. Now when this pulse, $P1$, is received and sampled it is easy to calculate the distance to the object from which the pulse has been reflected. Imagine again that a pulse, $P2$, is transmitted from the radar. After this, a pulse $X$ is received and the goal is to calculate the distance to the reflecting object. However, it is now not clear which of the reflections from pulses $P1$ or $P2$ that has been received. This leads to the realisation that the received pulse $X$ could have been reflected from objects at the distances $c\Delta t/2$ or $c(\text{PRI} + \Delta t)/2$. This gives the unambiguous range that can be measured as the following [14].

$$R = \frac{c}{2\text{PRF}} \tag{2.11}$$

*Doppler Ambiguities*
Doppler ambiguities or velocity ambiguities are also important effects that has to be kept in mind when developing radar systems. In order to understand why these ambiguities arise it is important to understand how the Doppler shift is measured in a radar. Doppler shift is measured in *slow-time* which means that the frequency shift is measured between different pulses. This frequency shift arises from the Doppler effect which is visualised in figure 2.4.

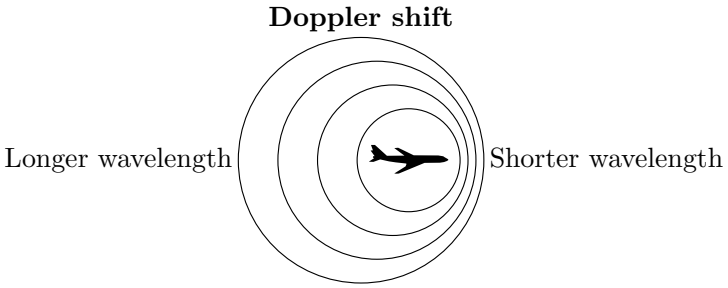


**Figure 2.4:** A visualisation of the Doppler effect. If a radar illuminates a moving object, say an aircraft, from every angle the reflection from said object will look like the one in this figure.

In the figure above we can imagine that the moving aircraft is omnidirectionally emitting electromagnetic waves. The figure above shows the pattern that arises due to the velocity of the aircraft. In front of the airplane the frequency of the waves will be higher than in the back. This is due to the fact that the aircraft is moving forward. The frequency shift from the waves reflected on the ground can now be calculated as the difference between the frequency of the transmitted signal and the received signal. This difference can be denoted by $f_d$ and the radial velocity can be calculated as

$$v_r = \frac{\lambda f_d}{2}. \tag{2.12}$$

However, if the target is not right in front of the radar but rather at an angle, such as $\theta$ in figure 3.3, the equation above instead becomes

$$v_r = \frac{\lambda f_d}{2\cos(\theta)} \tag{2.13}$$

By theorem 3.1.1 the maximum positive and negative Doppler shifts that can unambiguously be calculated is given by $\pm\text{PRF}/2$ (this is also called the Nyquist criterion [18]). Now combining these two ambiguities we get

$$R_{\text{maximum}} = \frac{c}{2\text{PRF}}, \tag{2.14}$$

$$f_{d,\text{maximum}} = \pm\frac{\text{PRF}}{2}. \tag{2.15}$$

As can be seen above these two are inversely proportional to each other which means that if the unambiguous range is increased the unambiguous Doppler frequency will decrease. This becomes a problem since there is no PRF which maximizes unambiguousness in both range and Doppler.

# 3
# Signal Processing

In the following sections both basic signal processing theory and more advanced MIMO theory is presented. Initially, digital filters is presented and later on MIMO waveforms is presented. The aim of this chapter is to further the theoretical framework needed to understand results from this study.

## 3.1 Basic Signal Processing

As mentioned above a signal is any measurable quantity that carries information. In order to decode or understand this information there are several useful techniques, some of which will be explained in this chapter. There are a few different ways of representing signals; however, in order for a signal to be processed digitally it has to be discretised both in amplitude and in time [14].

The fact that it is actually possible to discretise a signal without aliasing (a type of distortion) has been proved by Shannon in [19] with the following theorem.

**Theorem 3.1.1 (Shannon's Sampling Theorem)** *If a function $f(t)$ contains no frequencies higher than $W$ cps, it is completely determined by giving its ordinates at a series of points spaced $1/(2W)$ seconds apart.*

This is usually done by using an *analog-to-digital converter*, with which one can represent any signal as a vector of discrete values such as in equation (3.1).

$$\mathbf{s} = \begin{bmatrix} s(t_1) \\ s(t_2) \\ \vdots \\ s(t_N) \end{bmatrix} \tag{3.1}$$

This is essential for any processing since this is the way a computer can process the information. But in order to actually gain any insight into the information carried by the signal one has to apply a selection of different signal processing techniques, some of which will be presented below.

### 3.1.1 The Discrete Fourier Transform

One of the most central theoretical parts of radar theory is the Fourier transform which is used to transform a signal from the time domain to the frequency domain.

This is useful when trying to decode a signal to a sum of its base signals i.e, a sum of sinusoidal waves. The Fourier transform, $\hat{f}(\xi)$, of $f(t)$ is given by the integral equation

$$\hat{f}(\xi) = \int_{-\infty}^{\infty} f(t) \exp\left(-i2\pi\xi t\right) dt. \tag{3.2}$$

In radar theory it is generally not the continuous case which is most useful but rather a discrete version, known as the discrete Fourier transform (DFT), which can be stated as

$$X_k = \sum_{n=0}^{N-1} x_n \exp\left(-i2\pi \frac{k}{N} n\right). \tag{3.3}$$

This is in general a time consuming calculation; however, one way of calculating this quickly is the fast Fourier transform (FFT). This is one of the building blocks of signal processing and will be used frequently in this study.

### 3.1.2 Optimal Detection

It can be shown that SNR has great impact on the performance of a radar system which is why this ratio should be maximised. One step on the way to maximising this can be done by using what is called a matched filter. It is possible to write the received power as

$$|y|^2 = \mathbf{w}^H \mathbf{z}\mathbf{z}^H \mathbf{w}, \tag{3.4}$$

where $\cdot^H$ denotes the Hermitian conjugate, $\mathbf{z}$ is the vector from equation (2.1) and $\mathbf{w}$ is the impulse response. In order to find the matched filter one wants to find the vector $\mathbf{w}$ which maximises SNR. In order to do this it is important to formulate the optimisation problem. This is given by

$$SNR = \frac{\mathbf{w}^H \mathbf{s}^* \mathbf{s}^T \mathbf{w}}{\mathbf{w}^H \mathbf{R_N} \mathbf{w}}. \tag{3.5}$$

In the equation above, $\mathbf{w}$ is the filter coefficient vector, $\mathbf{s}$ is the steering vector and $\mathbf{R_N}$ is the noise covariance matrix, which describes clutter, $\mathbf{c}$, and noise, $\mathbf{n}$, defined in equation (2.1). It is worth to note that $\mathbf{w}^H \mathbf{s}^* \mathbf{s}^T \mathbf{w}$ is the received signal power and $\mathbf{w}^H \mathbf{R_N} \mathbf{w}$ is the average noise power [14]. The maximum SNR is then given by

$$\mathbf{w} = k {\mathbf{R_N}}^{-1} \mathbf{s}^*, \tag{3.6}$$

for any $k$ (for entire derivation see [14]).

## 3.2 Waveform design

When designing radar systems an obvious question is what waveforms to use. This is a very complex question which will be examined in the following sections.

### 3.2.1 Pulse compression

As stated above range resolution is highly dependent on pulse width with an increasing resolution for a shorter pulse width and a decreasing resolution for longer pulse widths. Furthermore signal-to-noise ratio decreases with a shorter pulse width and increases with a longer pulse width. However, since in general, it is desirable to increase both at the same time this poses somewhat of a problem. A solution to this problem is pulse compression. Pulse compression can use any kind of signal modulation, some of which has has been explained in section 3.

*Linear FM waveform*
One important instance of pulse compression is the linear frequency modulated waveform which is sometimes referred to as a chirp. We can describe a chirp as

$$s(t) = \text{rect}\left(\frac{t-\tau_{sc}}{T_p}\right)\exp\left(j\pi\gamma(t-\tau_{sc})^2\right)e^{-j\omega_c(t-\tau_{sc})}, \tag{3.7}$$

where $t$ describes fast-time, $\tau_{sc}$ describes the time delay from transmit to receive which in turn corresponds to the range to target. The function $\text{rect}(x)$ is defined as

$$\text{rect}(x) = \begin{cases} 1 & \text{if } |x| \leq 1/2 \\ 0 & \text{if } |x| > 1/2 \end{cases} \tag{3.8}$$

Furthermore $T_p$ denotes the pulse width, $\gamma$ denotes the chirp rate and $\omega_c = 2\pi f_c$ where $f_c$ is given by the frequency of the carrier wave. Worth to note is that this can be understood as a sinusoid whose frequency changes like the one shown in figure 2.1. We can now describe the waveforms from each antenna as a matrix were every column $i$ corresponds to the waveform for antenna element $i$ [20].

### 3.2.2 MIMO waveforms

There are multiple available types of MIMO waveforms and only some of them are appropriate for radar purposes. According to Bergin and Guerci in "MIMO Radar Theory and Application" there are primarily three types of diversification methods: time domain waveform design, frequency domain waveform design and code domain waveform design [5]. This study will only examine a subset of these waveforms and in particular frequency division multiple access (FDMA) has been examined by producing different chirps for every antenna element. Every chirp has a carrier frequency and by shifting this carrier frequency between waveforms FDMA is created. There are multiple ways of creating orthogonal waveforms this way; however, the most straightforward way is probably to separate the waveforms enough for no part of each waveform to overlap [5].

Another important effect of using MIMO compared to SIMO is the fact that energy will be dispersed wider than in the SIMO case, meaning that the orthogonal MIMO waveforms covers an area $N_k$ times larger, where $N_k$ is the number of transmitting antenna elements [21]. This means that a MIMO system can use a larger part of

CPI's in one direction compared to a conventional which needs to split CPI's between the different look angles.

In order to classify how correlated MIMO waveforms are, a correlation matrix is used to visualise this. Notice that the name correlation matrix is used in spite of there being no stochastic element present. An example of such a covariance matrix´, $\mathbf{R_{wf}}$, is shown in the figure below which has been calculated using equation

$$\mathbf{R_{wf}} = \mathbf{S_{wf}}\overline{\mathbf{S_{wf}}}, \tag{3.9}$$

where $\mathbf{S_{wf}}$ is the waveform matrix from equation (3.16).

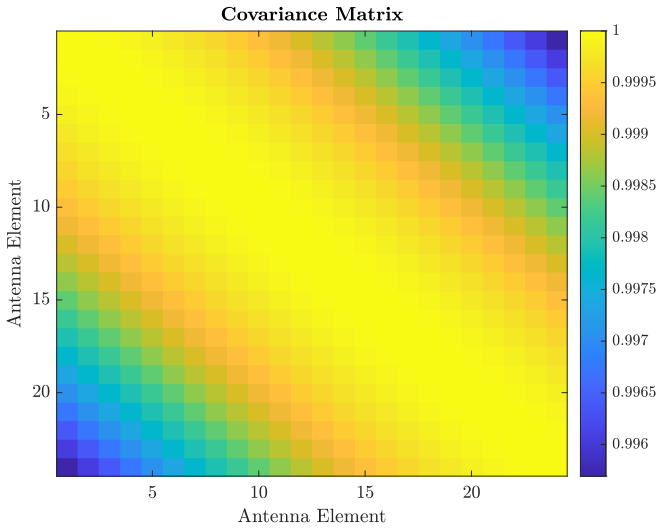


**Figure 3.1:** Correlation matrix for a 24 antenna element array. The value 1 means perfect correlation, or in this case the same waveform. The value 0 means that the waves are orthogonal. This covariance matrix corresponds to a system which is close to SIMO.

This matrix shows a model where the waveforms are close to SIMO. Fully, or close to fully orthogonal waveforms will instead generate a covariance matrix with the following appearance.

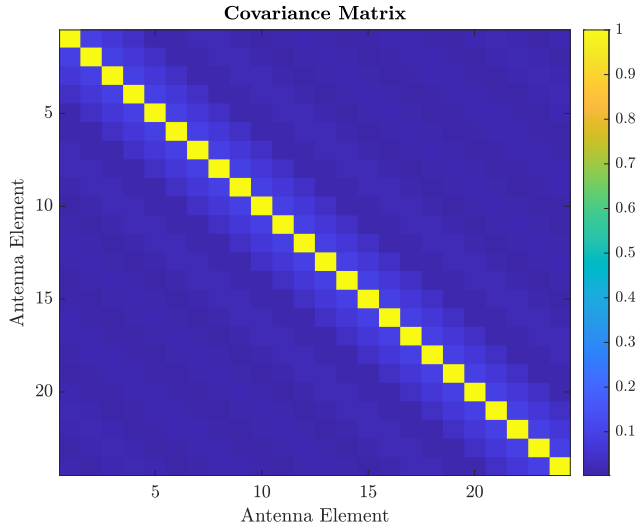


**Figure 3.2:** Correlation matrix for a 24 antenna element array. The value 1 means perfect correlation, or in this case the same waveform. The value 0 means that the waves are orthogonal. The figure above depicts a system which is close to orthogonal.

All of the above mentioned MIMO waveforms has been fast-time diversification i.e., in the same pulse. It is however, possible to think of diversification in slow-time as well, meaning between pulses. This way it is possible to decrease range ambiguities since one would know which pulse was sent at which time.

## 3.3 Space-Time Processing for GMTI

A technique used to manage clutter is called space-time processing which in short is a way of combining the space and time dimensions to reduce signals from unwanted reflections from the surrounding environment. This will be examined in the following sections by intertwining modelling of clutter and use of STP to manage the effects of clutter.

### 3.3.1 Clutter Modelling

Radars can be used to identify objects. However, some objects are of interest and some are not. The idea is that responses, or reflections, from objects that are of interest should be strong and responses from objects that are not of interest should be weak. The responses from objects that are not of interest is what is called clutter. Clutter from the ground i.e., any reflection from anything stationary on the ground, is spread out in both space and time if the radar is moving. Given this it is very difficult to mitigate clutter if only either the space or time domain is processed. However, if space and time is combined when processing it is possible to extract more useful information [7].

In order to model clutter it can be approximately described as a number of point scatterers. The return from these point scatterers can be described using steering vectors. There are different types of steering vectors, on the receiving side one spatial and one temporal. Given an array of $N_k$ antenna elements with spacing $l_u$, which often is chosen as $\lambda/2$, where $\lambda$ is the carrier wavelength, one can calculate the complex gain for antenna $i$ as

$$a(i) = e^{-2\pi f_u(i-1)} \tag{3.10}$$

where $f_u$ is the spatial frequency given by equation (3.11).

$$f_u = \frac{l_u}{\lambda}\sin\theta = \frac{\lambda}{2\lambda}\sin\theta = \frac{1}{2}\sin\theta \tag{3.11}$$

Now the spatial steering vector, which represents the phase delays at every antenna element for an incoming plane wave, for each point scatterer can be defined as

$$\mathbf{s}(f_u, N_k) = \begin{bmatrix} 1 & e^{-j2\pi f_u} & e^{-j4\pi f_u} & \cdots & e^{-j2\pi(N_k-1)f_u} \end{bmatrix}^T. \tag{3.12}$$

Equation (3.12) is representing the phase shift presented as a result of the angle of arrival (AoA) of the plane wave. In figure 3.3 an incoming plane wave is shown and the phase shift is shown as the distance from the plane wave to the antenna element at the time when the plane wave hits the first antenna element [5].

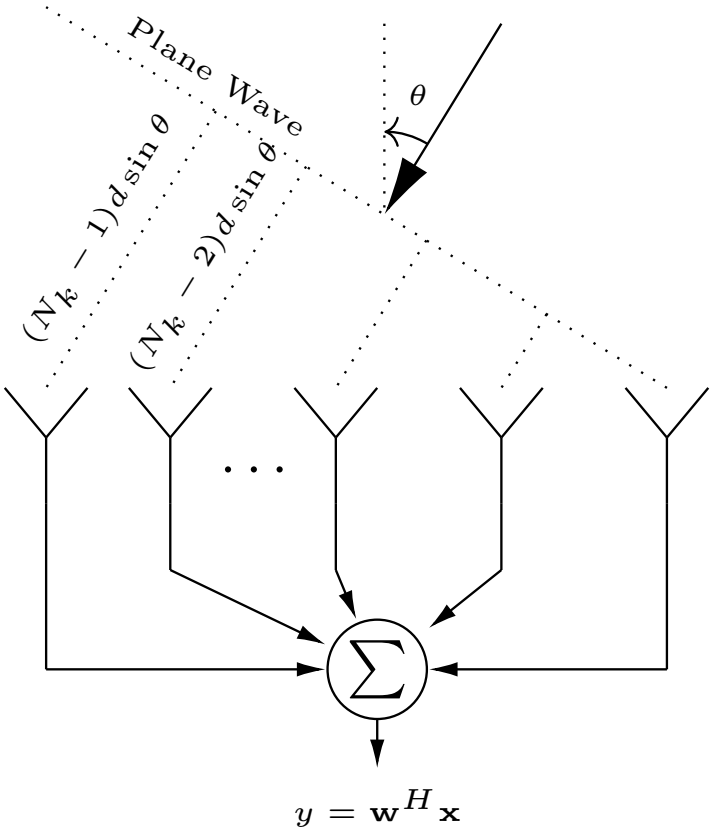


**Figure 3.3:** The figure depicts an incoming plane wave with angle of arrival (AoA) $\theta$ which is received by a uniform linear array with $M$ receivers. (After [5].)

The Doppler steering vector is given by the same Vandermonde vector as in equation (3.12) with the exception that the spatial frequency $f_u$ is exchanged with a normalised Doppler frequency $f_d$ given by

$$f_d = \frac{2v_p}{\lambda \cdot \mathrm{PRF}}. \tag{3.13}$$

To obtain the space-time steering vector $s_{st}$ the Kronecker product between the spatial and Doppler steering vectors are calculated which gives

$$\mathbf{s}_{st,RX} = \mathbf{s}(f_d, N_p) \otimes \mathbf{s}(f_u, N_k), \tag{3.14}$$

where $\mathbf{s}(f_d, M)$ and $\mathbf{s}(f_u, M)$ are defined by equation (3.12). Notice that there is one space-time steering vector corresponding to every point scatterer. In the equations above it is only the receiving end that has been taken into account. To make the model more complete TX has to be accounted for as well. In order to find the space-time steering vector for the transmitting side one needs to take the waveforms into account. Given, for example, a linear FM wave which can be described as

$$s(t) = \mathrm{rect}\left(\frac{t-\tau}{T_p}\right) \exp\left(j\pi\gamma(t-\tau)^2\right), \tag{3.15}$$

a waveform matrix of waveform vectors can be constructed as

$$\mathbf{S_{wf}} = \begin{bmatrix} \mathbf{s_0} & \mathbf{s_1} & \mathbf{s_2} & \cdots & \mathbf{s_{N-1}} \end{bmatrix}. \tag{3.16}$$

Furthermore a steering vector for the spatial dimension can be introduced for the transmit side as well. This steering vector will however be chosen as the same as for the receiving side i.e., given by equation (3.12). Combining these two vectors by matrix multiplication the following transmit waveform vectors is obtained [20].

$$\mathbf{s_{st,TX}} = \mathbf{S}_{wf}\mathbf{b}_{TX} \tag{3.17}$$

The equation above is hence the waveform experience by the environment in the direction given by angle $\theta$. By combining transmit and receive the total steering vector is obtained as

$$\mathbf{s}_{\text{st,total}} = \mathbf{s}_{\text{st,TX}} \otimes \mathbf{s}_{\text{st,RX}} = (\mathbf{s}_{\text{wf}}\mathbf{b}_{\text{TX}}) \otimes (\mathbf{s}(f_u, N_k) \otimes \mathbf{s}(f_d, N_k)). \tag{3.18}$$

Once the total steering vector has been calculated it is possible to find the covariance matrix by first defining as the sum over all point scatterers given by

$$\mathbf{x} = \sum_{i=0}^{N_s-1} \alpha_i \mathbf{s}_{\text{st},i}, \tag{3.19}$$

With $\mathbf{s}_{\text{st},i}$ being the space-time steering vector corresponding to clutter patch $i$ and $\alpha_i$ being a complex circularly-symmetric Gaussian random variable with mean 0. Further more $\alpha_i$ has has the covariance

$$\mathrm{E}\left[\alpha_i \alpha_j^H\right] = \begin{cases} \sigma_0 & \text{if } j = i \\ 0 & \text{if } j \neq i. \end{cases} \tag{3.20}$$

In the equation above $\sigma_0$ is the radar cross section which is a constant that takes into account how much reflection there is from an object. This has been assumed to have the value 1. Then one can write

$$\mathrm{Cov}\left(\mathbf{x}, \mathbf{x}^H\right) = \mathbb{E}\left[\mathbf{x}\mathbf{x}^H\right] - \mathbb{E}\left[\mathbf{x}\right]\mathbb{E}\left[\mathbf{x}^H\right] = \mathbb{E}\left[\mathbf{x}\mathbf{x}^H\right], \tag{3.21}$$

where the second equality holds since $\mathbf{x}$ is zero mean. By definition the expectation can be approximated by the sum

$$\mathbb{E}\left[\mathbf{x}\mathbf{x}^H\right] = \mathbb{E}\left[\sum_i \sum_j \alpha_i \alpha_j^H \mathbf{s}_i \mathbf{s}_j^H\right] = \sum \sigma_0 \mathbf{s}_{\text{st}} \mathbf{s}_{\text{st}}^H = \sum \mathbf{s}_{\text{st}} \mathbf{s}_{\text{st}}^H, \tag{3.22}$$

In the case of a uniform linear array one obtains the following equation for the covariance matrix

$$\mathbf{R}_c = \frac{1}{N_S}\mathbb{E}\left[\mathbf{x}\mathbf{x}^H\right] = \frac{1}{N_s}\sum \mathbf{s}_{\text{st}} \mathbf{s}_{\text{st}}^H, \tag{3.23}$$

where $1/N_s$ is a normalisation factor. This equation for the entire covariance matrix can be written as $\mathbf{R} = \mathbf{R_c} + \mathbf{R}_{\text{thermal}}$ where $\mathbf{R_c}$ corresponds to the sum in equation (3.23) and $\mathbf{R}_{\text{thermal}} = \sigma_n^2 \mathbf{I}$ with $\sigma_n^2$ being the variance which for white noise is equal to 1. In order to calculate the entire covariance matrix the the following can be used

$$\mathbf{R} = \frac{1}{N_s} \sum_{l=0}^{N_s-1} \mathbf{s}_{st} \mathbf{s}_{st}^H + \sigma_n^2 \mathbf{I}, \tag{3.24}$$

where the assumption $\sigma_0 = 1$ has been made. In order to examine the resilience of a radar to clutter a suitable approach is to calculate performance metrics such as the signal-to-interference plus noise ratio or the clutter-and-noise power which will be done below [22].

### 3.3.2 Performance metrics

There are several possible performance metrics available but some of the most common are *signal-to-noise ratio*, *signal-to-interference plus noise ratio* and *clutter-and-noise power (CP)*. This study focuses mainly on SINR and CP where SINR is calculated by distributing synthetic targets and evaluating the ratio of signal-to-interference and noise which can be written as

$$\text{SINR} = \frac{\mathbf{s}}{\mathbf{c} + \mathbf{n}}, \tag{3.25}$$

where $\mathbf{s}$ is the signal, $\mathbf{c}$ denotes the interference and $\mathbf{n}$ represent the noise. CP on the other hand is a measure of how much clutter the radar receives. The evaluation of CP is similar to that of SINR with the exception that the covariance matrix is not inverted which can be seen in the equation below. These ratios have been chosen because of their relevance to radar performance and their relatively simple implementation. Using theory developed in previous sections it is, given that it is possible to calculate the covariance matrix, feasible to calculate SINR and CP as

$$\text{SINR} = \mathbf{s_{st}}^H \mathbf{R}^{-1} \mathbf{s_{st}}, \tag{3.26}$$

$$\text{CP} = \mathbf{s_{st}}^H \mathbf{R} \mathbf{s_{st}}. \tag{3.27}$$

The metrics above exist for every target, e.g., SINR exists for every simulated target. It is worth to note that SINR comes from the case of matched filtering, see equation (3.6), where in this study $\alpha$ is assumed to be 1 which does not affect neither SINR nor CP. Furthermore these performance metrics are multidimensional, meaning that they can be calculated for different dimensions. Let's look at an example: Imagine a two dimensional grid with every point corresponding to an angle and a range. It is now possible to, by choosing $\mathbf{s_{st}}$ such that only range and angle is included, calculate a SINR value for every point on this grid. However, it is also possible to include a velocity for each and every point scatter such that there is now three dimensions available and SINR can then be calculated for any combination of these dimensions. A theoretical example of how such a SINR plot may look in two dimensions is shown in the figure below.

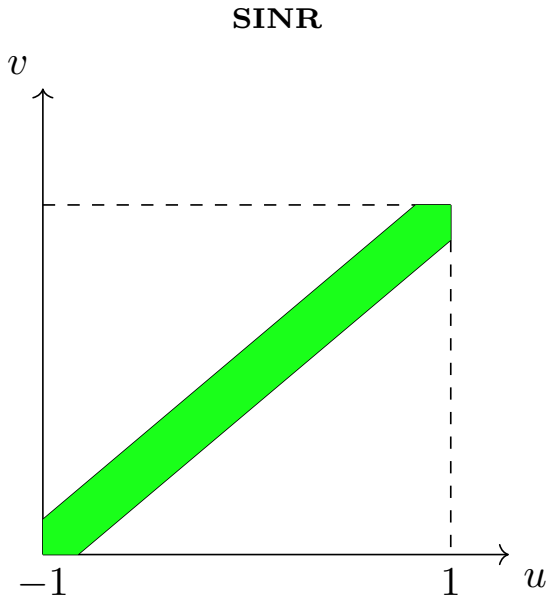


**Figure 3.4:** The MDV for a specified acceptable SINR loss is visualised as the width of the clutter ridge shown in this figure.

Another performance metric is the so called minimum detectable velocity. This is a measure of how slow objects the radar is able to detect and it can be found by intersecting SINR in Doppler-Azimuth for a given angle. In figure 3.5 an intersection of a SINR plot is shown.

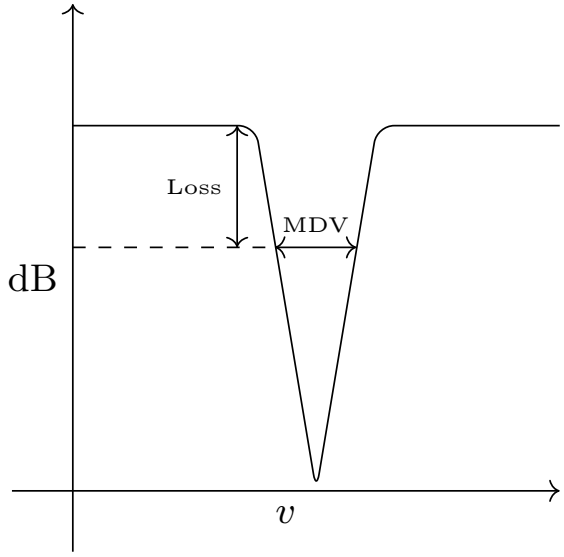


**Figure 3.5:** The MDV for a specified acceptable SINR loss is visualised as the width of the clutter ridge shown in this figure.

In this study MDV will be an important evaluation metric; however, it is worth to again note that this metric is highly dependent on how large a loss one accepts.

### 3.3.3 A factor representation of the Covariance Matrix

As previously stated the covariance matrix becomes increasingly large when the size of a system increases. In order to still be able to simulate large systems one can use a factor representation of the covariance matrix. This is, in this report, done based on an unpublished manuscript, "A factor representation of clutter plus noise covariance matrices" written by Tomas McKelvey that deals with dimension reduction by utilising singular value decomposition [23]. This method works by exploiting the fact that only a small number of vectors approximately span the entire space of the matrix since the eigenvalues rapidly decrease towards zero. The original way of calculating the covariance matrix in this study was by using the

$$\mathbf{R} = \frac{1}{N_s}\sum_{l=1}^{N_s} \mathbf{s}_{st}\mathbf{s}_{st}^H \ + \sigma_n^2\mathbf{I}, \tag{3.28}$$

notice that the RCS is not taken into account, this is a limitation of the study.

One way of implementing this dimensionality reduction, to approximate the covariance matrix above, is by using singular value decomposition (SVD) to create a low rank approximation of the covariance matrix [24]. This is done by first decomposing the matrix $\mathbf{S}_{st}$ consisting of space-time steering vectors $\mathbf{s}_{st}$ which can be defined as

$$\mathbf{S}_{st} = \begin{bmatrix} \mathbf{s}_{\mathrm{st},1} & \mathbf{s}_{\mathrm{st},2} & \cdots & \mathbf{s}_{\mathrm{st},N_s} \end{bmatrix}, \tag{3.29}$$

with $N_s$ denoting the number of point scatterers. Then this matrix can be decomposed as

$$\mathbf{S}_{st} = \mathbf{U}\mathbf{\Sigma}\mathbf{V} = \sum_{i=1}^{r} s_i\mathbf{u}_i\mathbf{v}i^H, \tag{3.30}$$

where the matrix $\mathbf{\Sigma}$ is a diagonal matrix containing the singular values of $\mathbf{s}_{st}$, $s_i$ are the singular values, $\mathbf{U}$ and $\mathbf{V}$ is are complex valued unitary matrices. The integer $r$ denotes the effective numerical rank. This is chosen by using every normalised singular value over a threshold $\kappa$. Now we have that

$$\mathbf{R_c} = \frac{1}{N_s}\mathbf{S}_{st}\mathbf{S}_{st}^H = \frac{1}{N_s}\mathbf{U}\left(\mathbf{\Sigma}\mathbf{\Sigma}^H\right)\mathbf{U}^H, \tag{3.31}$$

where $1/N_s$ is a normalisation factor. The idea is now to only use vectors corresponding to all singular values above a certain threshold. By defining a unitary matrix $\mathbf{U}$ with $\mathbf{U} = [\mathbf{U}_1\mathbf{U}_1]$ with $\mathbf{U}\mathbf{U}^H = \mathbf{U}^H\mathbf{U} = \mathbf{I}$ [23]. As previously stated the total covariance matrix is given by $\mathbf{R} = \mathbf{R}_c + \sigma^2\mathbf{I}$ which in this case gives

$$\mathbf{R} = \mathbf{R_c} + \sigma^2\mathbf{I} \tag{3.32}$$

$$= \frac{1}{N_s}\sum_{i=1}^{r} s_i^2\mathbf{u}_i\mathbf{u}_i^H + \sigma^2\mathbf{I} \tag{3.33}$$

$$= \frac{1}{N_s}\mathbf{U}\mathrm{diag}\left(s_1^2+\sigma_n^2, ..., s_r^2+\sigma_n^2, \sigma_n^2, ..., \sigma_n^2\right)\mathbf{U}^H, \tag{3.34}$$

where the second equality hold because of equation (3.31). Now putting this together we can write

$$\text{CP} = \mathbf{s^H R s} = \mathbf{s^H U_1} \text{diag}(s_1^2, ..., s_N^2)\mathbf{U}_1^H\mathbf{s} + \sigma_n^2\mathbf{s}^H\mathbf{s}. \tag{3.35}$$

The expression for SINR, which is calculated using the inverse covariance matrix, is obtained as

$$\text{SINR} = \mathbf{s^H R}^{-1}\mathbf{s} = \mathbf{s^H U_1} \text{diag}(\frac{1}{s_1^2+\sigma_n^2} - \frac{1}{\sigma_n^2}, ..., \frac{1}{s_N^2+\sigma_n^2} - \frac{1}{\sigma_n^2})\mathbf{U}_1^H\mathbf{s} + \frac{1}{\sigma_n^2}\mathbf{s}^H\mathbf{s}. \tag{3.36}$$

# 4
# Simulation

This chapter presents methods used to produce results generated in this study. These methods are all built upon above presented theories. This chapter first presents a general antenna model used after which a clutter model is presented. Finally, different collections of waveforms and performance metrics is presented before moving onto results.

## 4.1 Antenna Model

Since the objective of this study is to evaluate possibilities of using MIMO waveforms to decrease MDV the main intent is to compare different types of waveforms. However, differently sized antennas are also of great interest which is why two differently sized antennas have been compared. The antenna model used throughout this study has been a uniform linear array. This type of array has been visualised in figure 3.3. Regarding different sizes, arrays with 4 and 24 antenna elements has been simulated. This would, given a carrier frequency of 3 GHz and a separation between elements of $\lambda/2$, amount to array lengths of 15 cm and 120 cm.

Furthermore different integration times i.e., different number of pulses have also been used ranging from 8 to 48 pulses. This has been varied both with regards to the same setup but also as to compare different beamforms since a wider beam can afford to use a greater number of pulses to scan the same area than a thinner beam, given a constant PRF. The airborne antenna is modelled in two dimensions, meaning that the elevation angle between ground clutter and antenna is assumed to be zero at all times.

### 4.1.1 Clutter Modelling

In order to calculate metrics such as SINR or CP it is necessary to calculate the clutter covariance matrix which as stated above can be done by assuming that clutter can be modelled as a cluster of point scatterers described by steering vectors. In order to calculate the clutter covariance matrix, 3600 synthetic point scatterers were randomly distributed in angle, distance and velocity. The point scatterers were distributed in 600 randomly chosen angles, 6 equally spaced distances between 2 km and 6 km and lastly every clutter point was associated with a Doppler frequency. It is worth to note that this is might be too few distances to assume that clutter

is homogeneous in distance. However, due to computational limitations it was not possible to simulate larger systems. Since clutter is stationary the received Doppler frequencies will be limited by the velocity of the radar platform and hence the perceived velocities are bounded by the platform velocity, $v_p$, as $-v_p \leq v_c \leq v_p$ where $v_c$ is the perceived clutter velocity.

Given this, one can calculate the covariance matrix by approximating the integral in equation (3.23) with a sum such as

$$\mathbf{R} = \sum_{l=0}^{N_s-1} \sigma_0 \mathbf{s}_{st} \mathbf{s}_{st}^H + \sigma_n^2 \mathbf{I}, \tag{4.1}$$

where $\sigma_0$ denotes the radar cross section, $\mathbf{s}_{st}$ is the total steering vector for a single point scatterer, $N_s$ is the number of point scatterers and lastly $\sigma_n^2$ is the thermal noise level. Worth to note is that the covariance matrix becomes very large very fast when increasing the number of antenna elements, the integration time or the number of fast-time samples. The size of the clutter covariance matrix is given by $N_r \cdot N_k \cdot N_p \times N_r \cdot N_k \cdot N_p$. For example, given a radar setup of 24 antenna elements, an integration time of 48 pulses a sampling frequency of 1 MHz and a pulse width of 10 $\mu$s, the clutter covariance matrix is built up of approximately 13 billion elements which in Matlab corresponds to 108 GB. This is in general too large for Matlab and it will increase run times or even provoke a crash.

Now in order to calculate performance metrics such as SINR it is necessary to distribute targets in all directions and velocities possible. This is because of the desire to find how much signal each target contributes with compared to other interferences at all possible points. In contrast to clutter distribution, which is random, target distribution has been performed uniformly between the unambiguous velocities which can be calculated as $v_r = \lambda \cdot \mathrm{PRF}/2$ which gives $-v_r/2 \leq v_{\text{target}} \leq v_r/2$. Targets are also distributed uniformly in direction.

### 4.1.2 Calculations of Performance Metrics

SINR and CP are calculated for each target, meaning that given 3600 targets with different angles and different velocities one can, for every target calculate SINR and CP as

$$\mathrm{SINR}_i = \mathbf{s}_{st,i}^H \mathbf{R}^{-1} \mathbf{s}_{st,i} \tag{4.2}$$

$$\mathrm{CP}_i = \mathbf{s}_{st,i}^H \mathbf{R} \mathbf{s}_{st,i}, \tag{4.3}$$

where $\mathbf{s}_{st,i}$ denotes the space-time steering vector, for each synthetic target and $\mathrm{SINR}_i$ denotes the signal-to-interference and noise ratio for target $i$. Worth to note here is that the right hand side is approxmiated using the factor representation explained above.

### 4.1.3 MIMO waveforms

In this study a few different types of MIMO waveforms has been used. In order to model such a case the so called waveform matrix, presented in equation (3.16), was introduced which is built up of rows corresponding to each fast-time time sample and columns corresponding to each antenna element or each waveform. This matrix is then combined together with a spatial steering vector to obtain a transmitting steering vector. Using the same receiving steering vector as with SIMO one can again calculate appropriate performance metrics.

Furthermore sparse arrays were investigated. Sparse means, in this context, that only a portion of the transmitting elements were actually emitting waveforms while the entire array was receiving. In this study a sparse array with 24 antenna elements was investigated by emitting waveforms from every fourth antenna element. In other words only 6 antenna elements were transmitting.

# 5
# Results

This chapter begins by presenting results from the baseline case of this study. This baseline setup includes two differently sized AESA using SIMO waveforms. Furthermore a selection of MIMO cases with the same antenna sizes as in the SIMO case will be presented as well. Finally the case of a sparse antenna will also be presented.

## 5.1 Illustration of Results

Results are mainly presented as figures illustrating a collection of performance metrics. These are SINR, CP, a cross section of SINR visualising the clutter ridge. Furthermore covariance matrices pertaining to the covariance between waveforms from different antenna elements will be displayed as well as a figure for antenna gain and one for the frequency sweep. Unless stated otherwise parameters will for each of the following results be constant. These parameters are shown in table 5.1.

| Parameter | Variable | Value | Units |
|---|---|---|---|
| Carrier frequency | $f_c$ | $3 \cdot 10^9$ | Hz |
| Pulse Repetition Frequency | PRF | $1 \cdot 10^4$ | Hz |
| Platform velocity | $v_p$ | 80 | m/s |
| Wavelength | $\lambda$ | $c/f_c$ | m |
| Element separation | $l_u$ | $5 \cdot 10^{-2}$ | m |
| Bandwidth | $B_p$ | $1 \cdot 10^6$ | Hz |
| Sampling frequency | $f_s$ | $1 \cdot 10^6$ | Hz |
| Pulse Width | $T_p$ | $1 \cdot 10^{-5}$ | s |

**Table 5.1:** Parameters for the general radar setup being simulated.

## 5.2 SIMO Waveforms

In this section results are obtained using SIMO waveforms and varying the number of pulses and antenna elements. In figure 5.1 below, subfigures are shown for an antenna with four elements emitting the same waveform from each antenna element i.e., SIMO waveforms. Figure 5.1a shows the frequency sweep of the waveform being emitted from every antenna element. In figure 5.1b the covariance matrix for waveforms is shown, since the waveforms are all the same the correlation between

them is one. In figure 5.1c the antenna gain is shown. Moving on SINR and CP are shown in figures 5.1d respectively 5.1e. Lastly the cross section along $u = 0$ in SINR is shown in figure 5.2f. The width of this ridge at a loss of 6 dB is how MDV is defined in this study. In this case MDV is 45.31 m/s. Every following result is built up this way. In figure 5.2 results from a SIMO simulation with 24 antenna elements and 48 pulses is shown. Although it is more difficult it is still possible to see the characteristic clutter ridge in both figure 5.2d and 5.2d.

## 5.3 Multiple-Input, Multiple-Output

In figures 5.3, 5.5 and 5.4 results from simulations using MIMO waveforms is presented. As before results are presented using ratios such as SINR and CP. To begin with, one can note that the frequency sweeps in every top left subfigure which shows how the frequency varies between the different waveforms. This is further visualised in the covariance matrix, which is the top right subfigure in every result figure. Pay attention to the fact that there are no longer as pronounced roots in neither SINR nor CP as there is when using SIMO waveforms.

It is important to note that MDV is calculated from the maximum value minus the loss in each particular case. This means that MDV is not calculated at the same absolute level in SIMO and MIMO since the energy is dispersed wider with MIMO waveforms. Take for example the 4 antenna element arrays. With MIMO waveforms the absolute level is approximately 6 dB lower than with SIMO waveforms. In other words SIMO has a higher sensitivity in absolute numbers. With 24 antenna elements this difference amounts to as much as 10 dB.

### 5.3.1 Sparse MIMO

Figure 5.6 presents results from using a sparse MIMO array meaning that only a portion of the antenna elements are transmitting while the entire array is receiving. In this case every fourth antenna element transmitted waveforms which where shifted in frequency to create orthogonal waveforms.

## 5.4 Summary

| Number of antenna elements | Waveform | Pulses | MDV (at 6 dB loss) |
|---|---|---|---|
| 4 | SIMO | 8 | 45.36 m/s |
| 4 | MIMO | 8 | 40.88 m/s |
| 4 | MIMO | 32 | 20.73 m/s |
| 24 | SIMO | 48 | 7.66 m/s |
| 24 | SIMO (Sparse) | 48 | 7.65 m/s |
| 24 | MIMO | 8 | 37.16 m/s |
| 24 | MIMO | 48 | 7.00 m/s |
| 24 | MIMO (Sparse) | 48 | 7.02 m/s |

**Table 5.2:** Table presenting results from simulations.

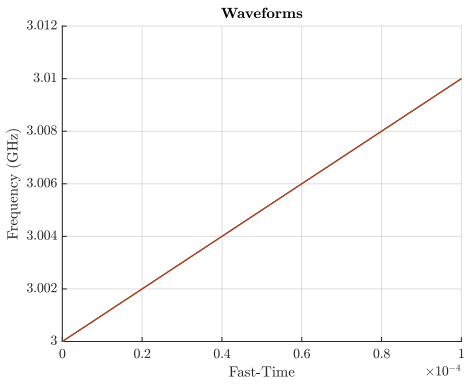


**(a)** LFM waveform

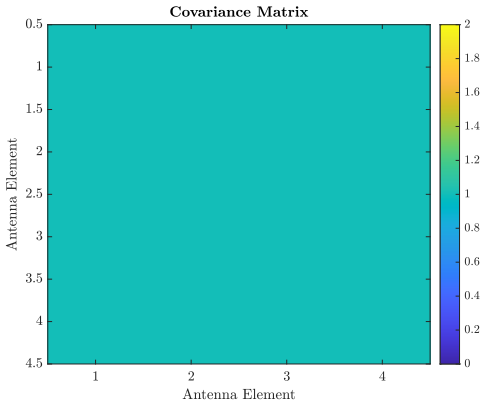


**(b)** Waveform Covariance Matrix

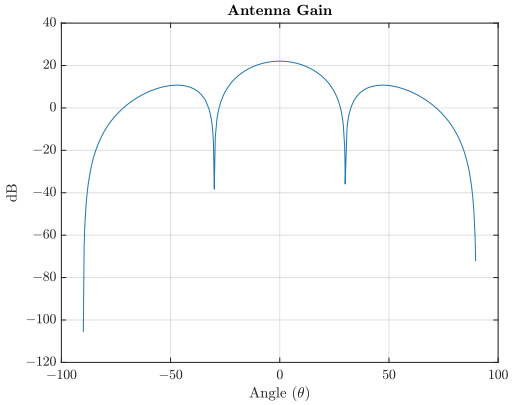


**(c)** Antenna Gain

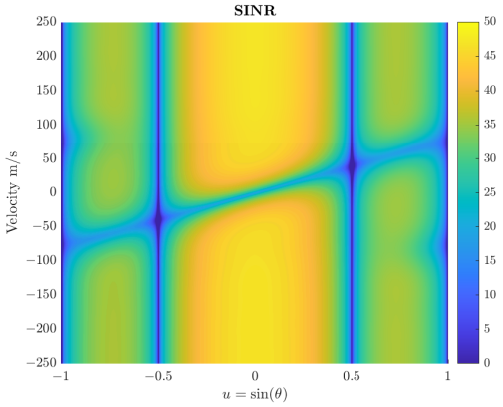


**(d)** SINR

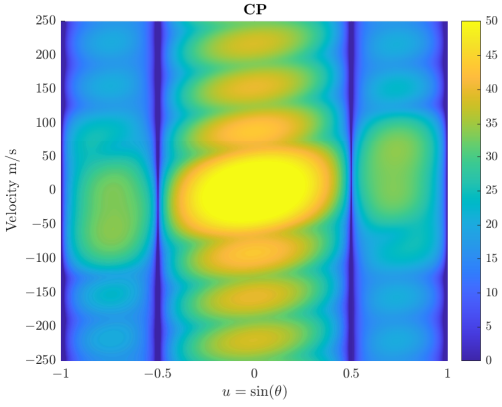


**(e)** CP

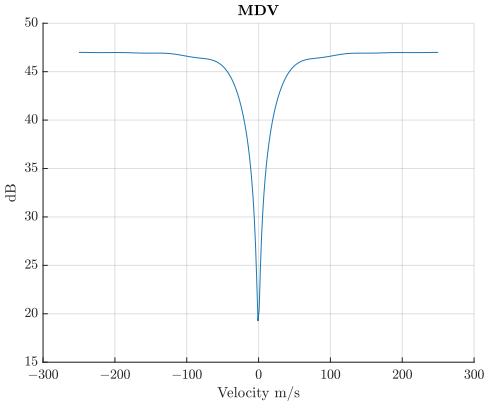


**(f)** MDV

**Figure 5.1:** Visualisation of results from simulation using SIMO waveforms meaning the same waveforms are emitted from every antenna element. In this case MDV is, at a loss of 6 dB, 45.36 m/s.

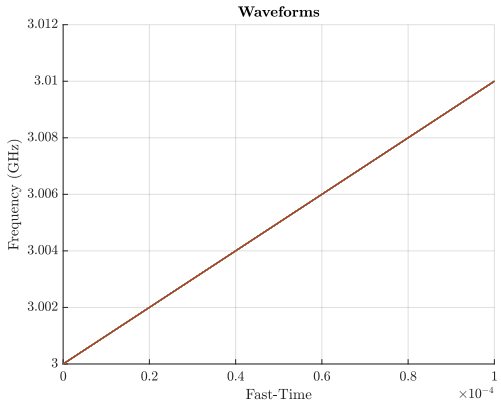


**(a)** LFM waveform

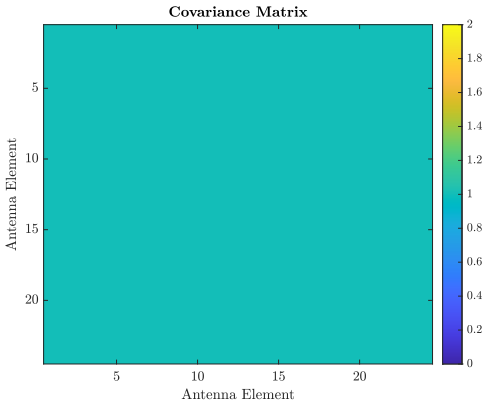


**(b)** Waveform Covariance Matrix

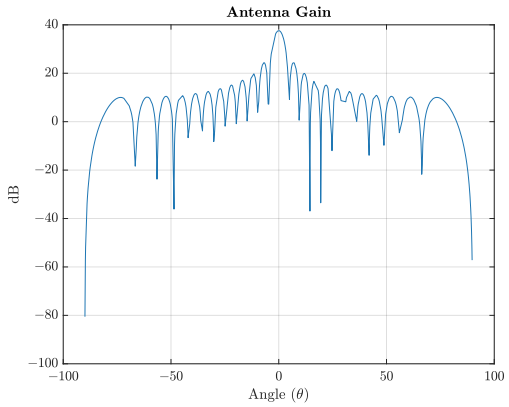


**(c)** Antenna Gain

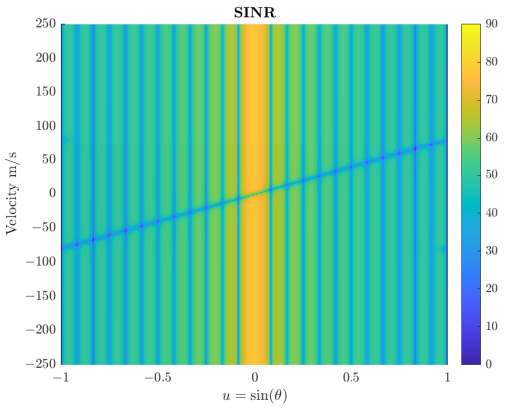


**(d)** SINR

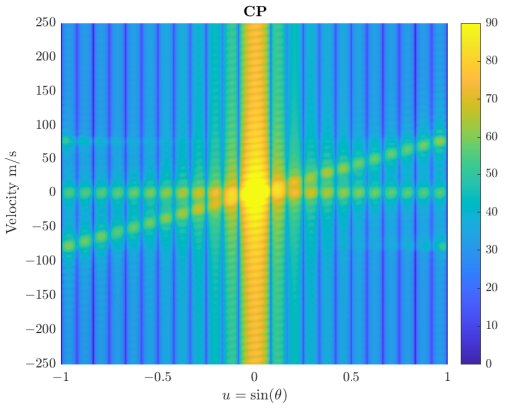


**(e)** CP

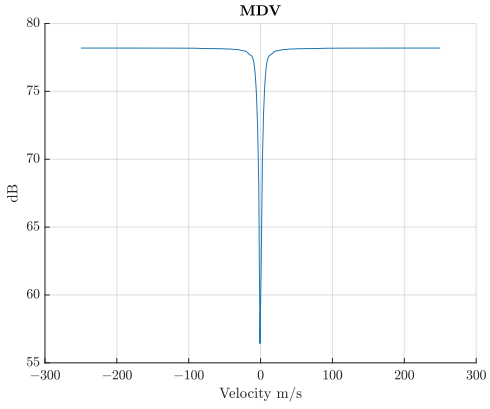


**(f)** MDV

**Figure 5.2:** Visualisation of results from simulation using SIMO waveforms, with 24 antenna elements, meaning the same waveforms are emitted from every antenna element. In this case MDV is, at a loss of 6 dB, 7.66 m/s.

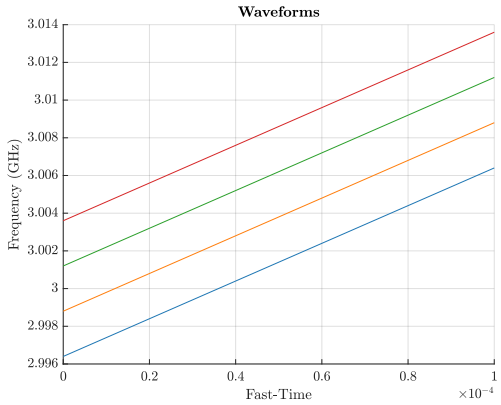


**(a)** LFM waveform

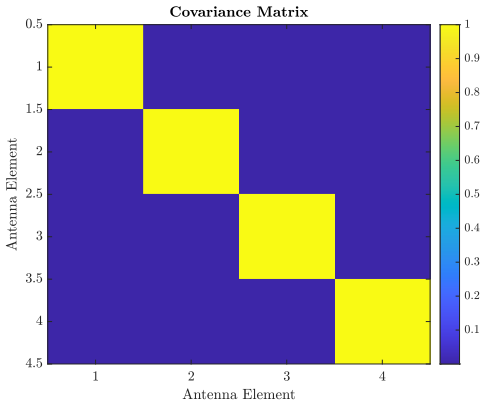


**(b)** Waveform Covariance Matrix

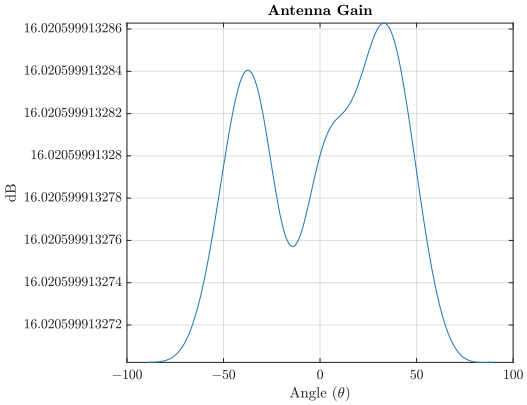


**(c)** Antenna Gain

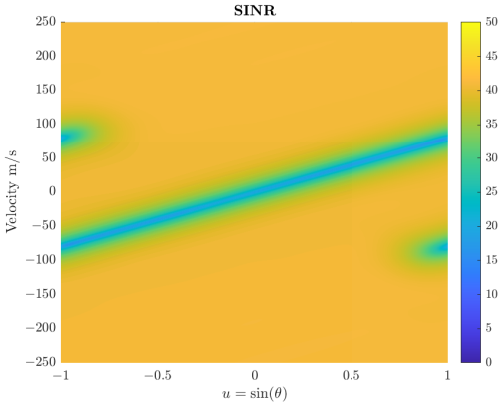


**(d)** SINR

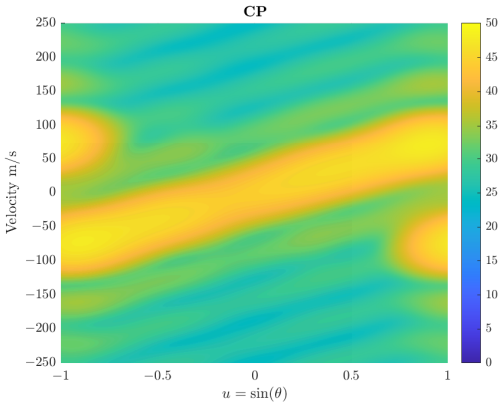


**(e)** CP

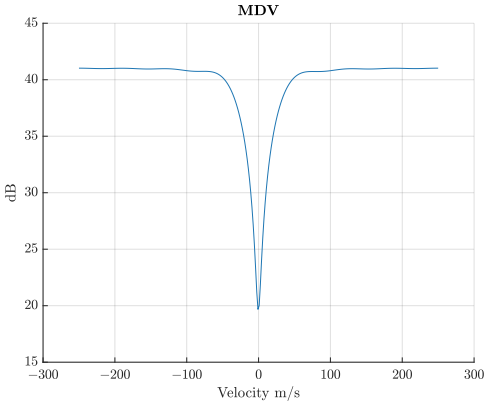


**(f)** MDV

**Figure 5.3:** Visualisation of results from simulation using MIMO waveforms meaning different waveforms are emitted from every antenna element. In this case MDV is, at a loss of 6 dB, 40.88 m/s.

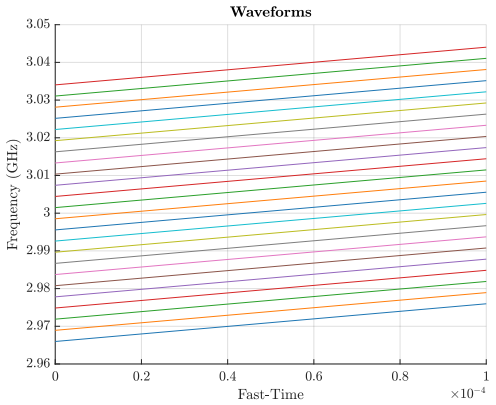


**(a)** LFM waveform

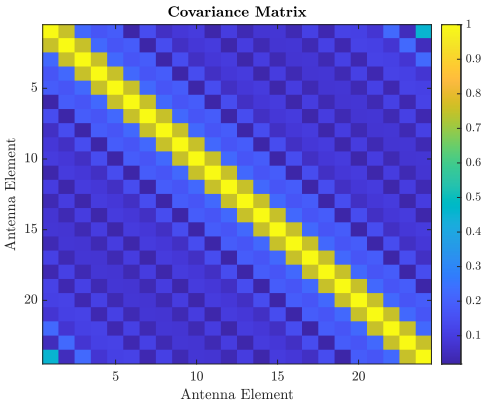


**(b)** Waveform Covariance Matrix

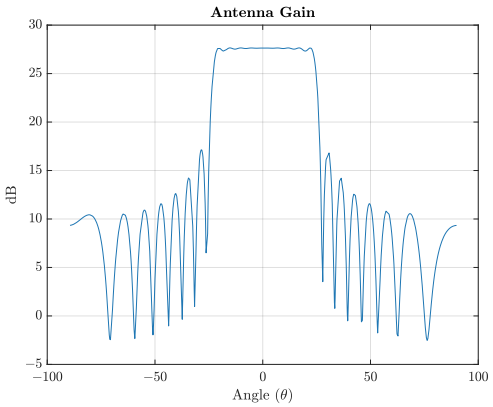


**(c)** Antenna Gain

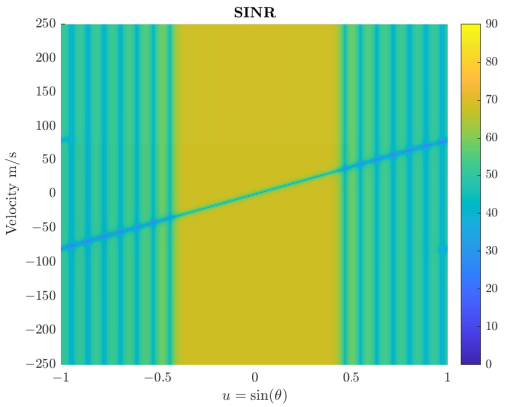


**(d)** SINR

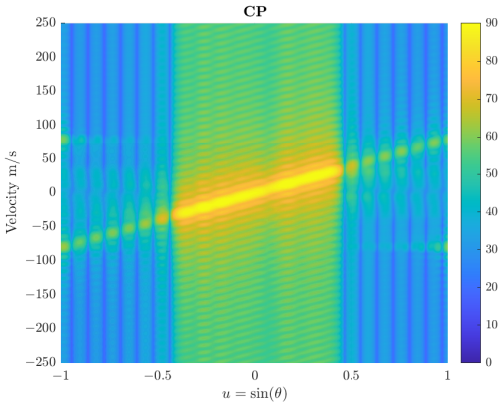


**(e)** CP

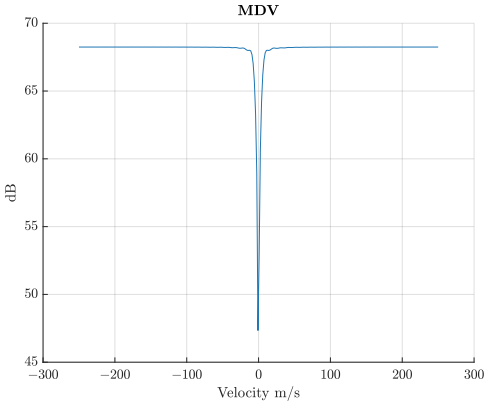


**(f)** MDV

**Figure 5.4:** Visualisation of results from simulation using MIMO waveforms meaning different waveforms are emitted from every antenna element. In this case MDV is, at a loss of 6 dB, 7.00 m/s.

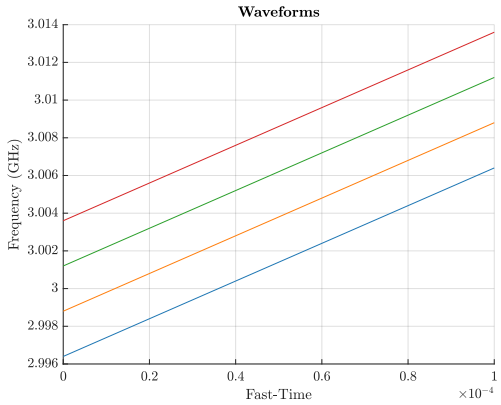


**(a)** LFM waveform

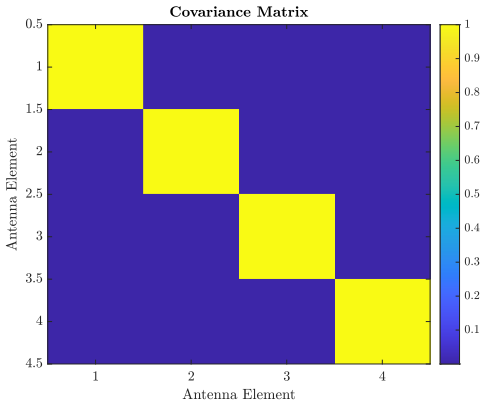


**(b)** Waveform Covariance Matrix

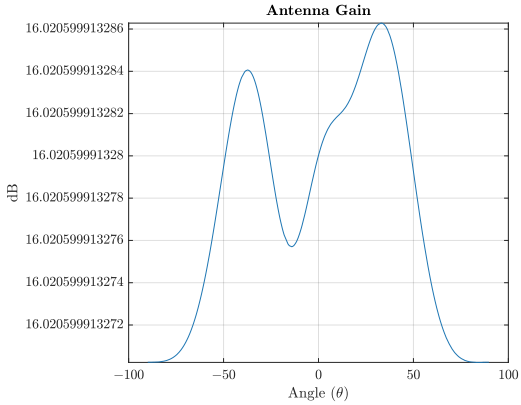


**(c)** Antenna Gain

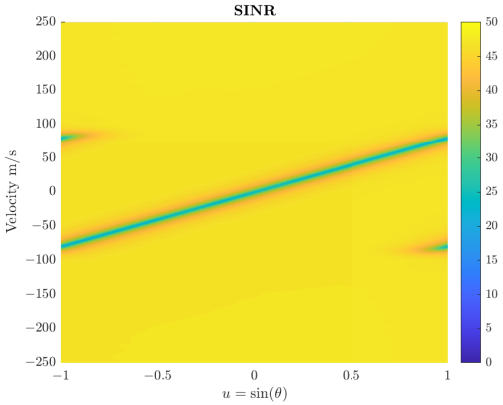


**(d)** SINR

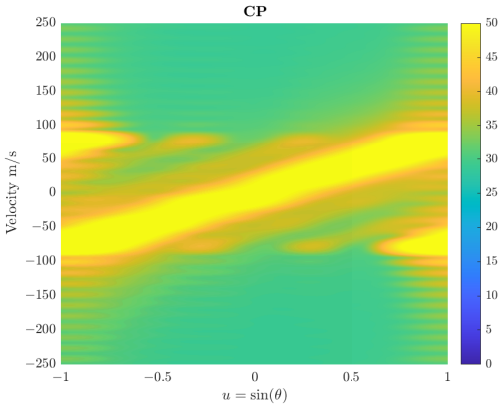


**(e)** CP

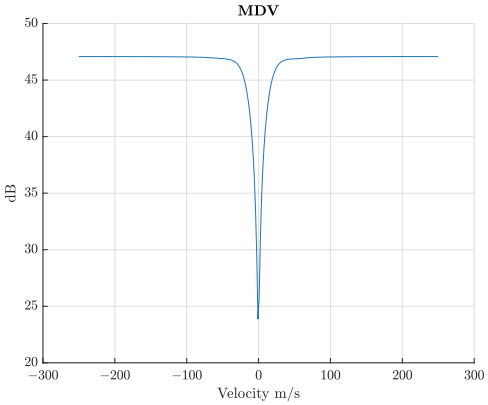


**(f)** MDV

**Figure 5.5:** Visualisation of results from simulation of a system comprised of 4 antenna elements and 32 pulses using MIMO waveforms. In this case MDV is, at a loss of 6 dB, 20.73 m/s.

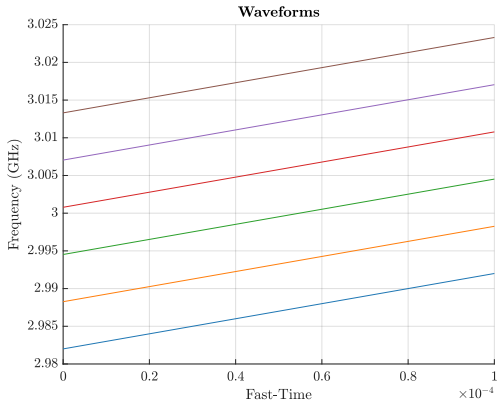


**(a)** LFM waveform

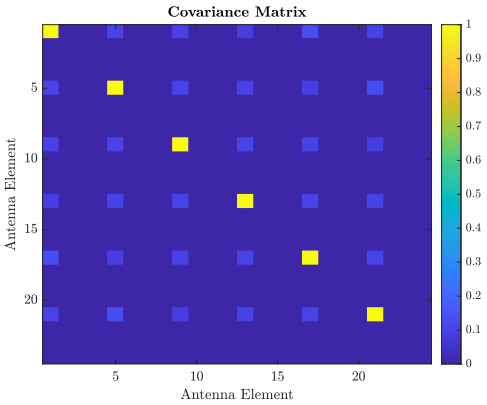


**(b)** Waveform Covariance Matrix

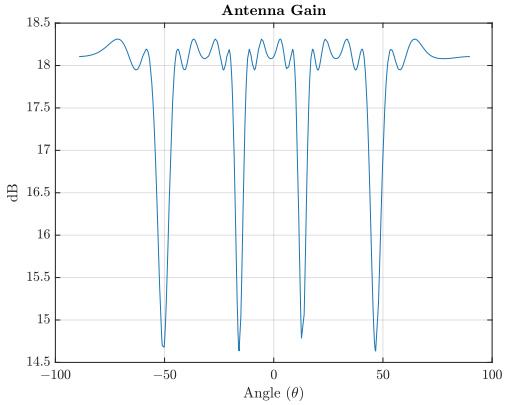


**(c)** Antenna Gain

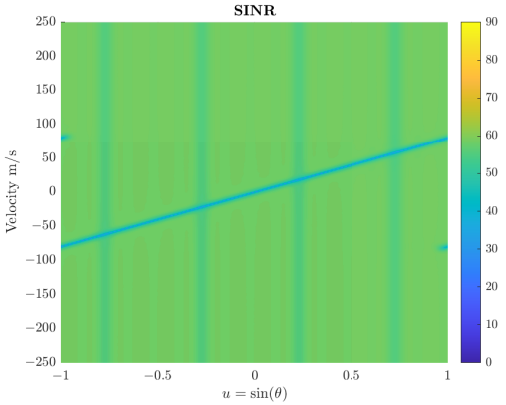


**(d)** SINR

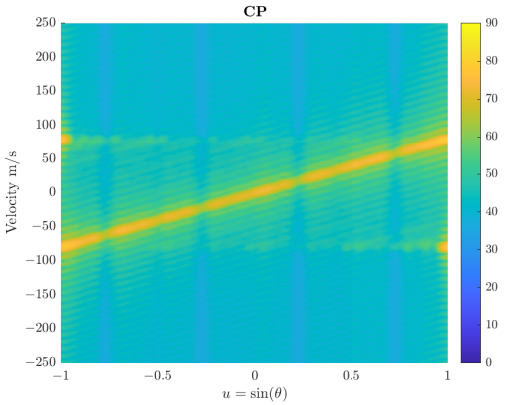


**(e)** CP

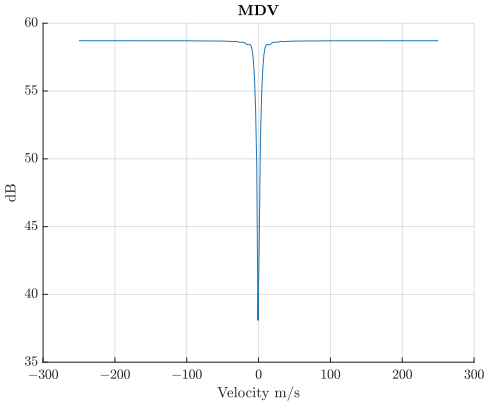


**(f)** MDV

**Figure 5.6:** Visualisation of results from simulation using sparse MIMO waveforms meaning waveforms are only emitted from every fourth antenna element with a frequency shift between every waveform. In this case MDV is, at a loss of 6 dB, 7.02 m/s.

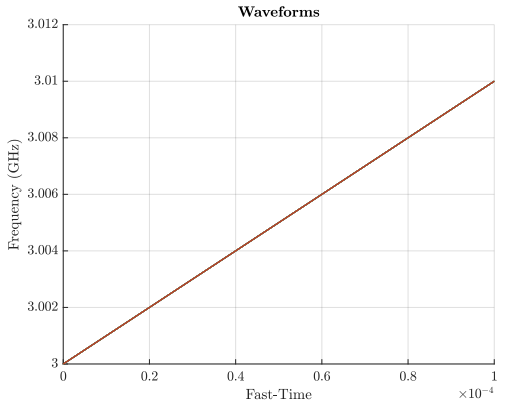


**(a)** LFM waveform

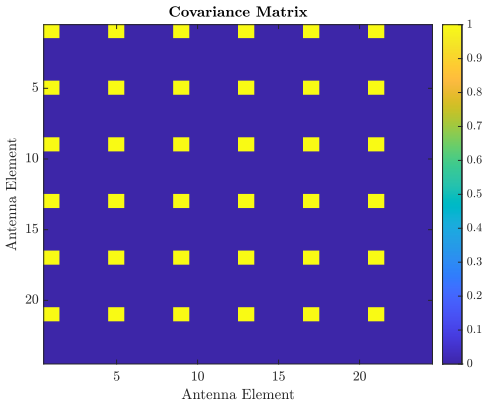


**(b)** Waveform Covariance Matrix

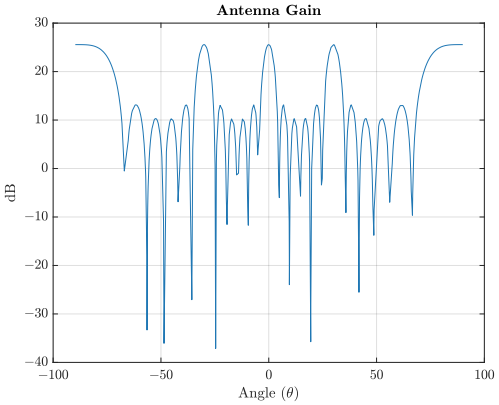


**(c)** Antenna Gain

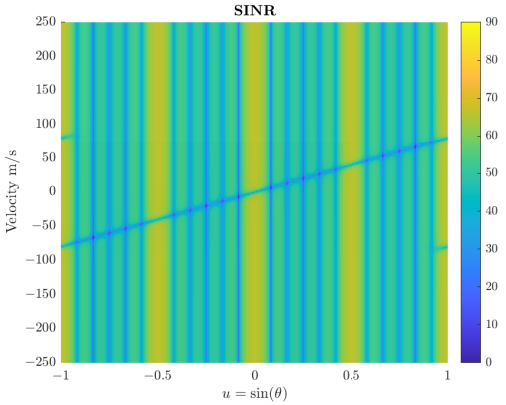


**(d)** SINR

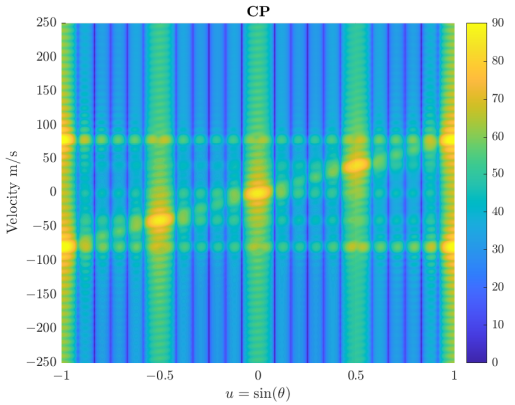


**(e)** CP

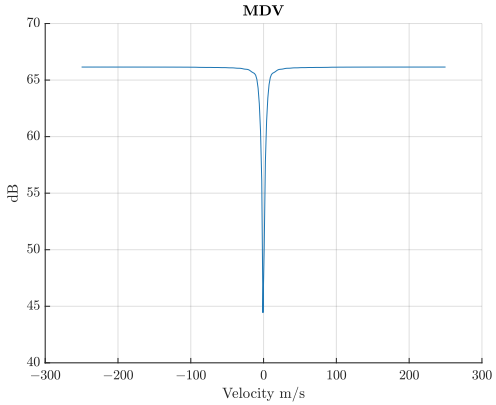


**(f)** MDV

**Figure 5.7:** Visualisation of results from simulation using sparse SIMO waveforms meaning waveforms are only emitted from every fourth antenna element without a frequency shift between every waveform. In this case MDV is, at a loss of 6 dB, 7.65 m/s.

# 6
# Discussion

This chapter will discuss results presented in the previous chapter. Comparisons have been made between arrays of equal size and between different types of waveforms and different number of pulses. Beginning with a small array and finalising with a larger array.

## 6.1 Small Array

The smaller array containing 4 antenna elements has as shown above been simulated using both MIMO and SIMO as well as different numbers of pulses. Regarding MIMO vs SIMO one can see that MDV is lower for the MIMO case; however, it is worth to note that MDV is calculated at different absolute values of SINR. This is because the loss is defined from the maximum value and therefore, because of the dispersion of energy in the MIMO case, the level at which MDV is measured will differ between the two cases. For example looking at figure 5.1f the maximum value is approximately 47 dB and in figure 5.3f the maximum value is 6 dB lower at approximately 41 dB. This means that MDV will be measured from different absolute SINR levels. However, since in the MIMO case it is possible to illuminate the same volume for a longer time the power would increase and therefore this comparison is deemed reasonable.

An example of this is shown in figure 5.5f where the same direction has been illuminated by 32 pulses instead of 8 which corresponds to the same volume being scanned in the same time as with SIMO. When doing this, MDV is decreased with as much as 20.15 m/s. This difference might seem large at first since increasing the number of pulses should only increase the resolution and not affect the clutter mitigation. However, if the minimum detectable velocity is bounded by the resolution, rather than the clutter ridge, this will be the effect.

## 6.2 Large Array

Moving on to the larger array consisting of 24 antenna elements with results in table 5.2 the same effect arises, which is that MIMO decreases MDV. Once again it is worth to note that the absolute value at which MDV is measured is lower in MIMO than in SIMO; however, the same argument as above holds. Due to restrictions in the simulation model and in hardware (RAM) it was not possible to simulate

systems larger than this which is why it is not possible to accurately estimate the results of a MIMO case with an appropriate number of pulses.

Furthermore one can look at the sparse arrays both in SIMO and in MIMO. In figure 5.6 neither SINR nor CP has changed a considerable amount compared to the full MIMO system in figure 5.4. However, looking at figure 5.7 blind-spots has arisen which are the brighter yellow lines shown. There are several possible pros with using a sparse array. One of the main pros is the decrease in cost since one does not need as many antenna elements to obtain the same result [25]. For example the antenna elements that is not used for GMTI can be used for other tasks such: for example jamming.

## 6.3 Simulation Model

This study has lead to the development of a model which is capable of simulating both MIMO and SIMO in the same model. This has several advantages compared to using different models for the two cases. For example in the book "Space-Time Adaptive Processing For Radar" SINR is calculated as

$$\text{SINR} = \mathbf{s}^H R^{-1} \mathbf{s}, \tag{6.1}$$

where $\mathbf{s} = \mathbf{a} \otimes \mathbf{b}$ where $\mathbf{a}$ is the Doppler Vandermonde steering vector and $\mathbf{b}$ is the spatial Vandermonde steering vector in which neither incorporates the transmit pattern [18]. In the model devoloped in this study one uses both the transmitting pattern and the receiving pattern, with both MIMO and SIMO, which leads to a more realistic model.

# 7
# Conclusion

There are multiple possible applications for MIMO waveforms in GMTI radars and one possible valuable assets is the fact that a MIMO radar can illuminate a fixed volume faster than a SIMO radar, meaning that the MIMO system can afford more pulses per direction. This in turn means that the Doppler resolution will increase and thereby the minimum detectable velocity can decrease as has been shown in the previous chapters. However, it is worth to note that since the antenna gain is lower overall in the MIMO case one will approximately end up at the same SINR level, which would indicate that this is not a valid argument for MIMO. On the other hand a sparse array which is utilising MIMO can, without a large loss in performance, put the other antenna elements to use in other tasks such as jamming.

One of the main results from this study is the framework built to simulate radar systems using MIMO, SIMO and sparse arrays in the same framework. This makes it possible to investigate different radar setups in the future, some of which are mentioned in the next section. This can be a valuable tool for research in the early stages.

## 7.1 Future work

There are countless possible extensions to this, some more interesting than others. However, one interesting extension would be to test the model on actual data that has been collected. Moreover it would be interesting to simulate different types of MIMO waveforms and in particular investigate the possibilities of slow-time MIMO (e.g. [26]).

Furthermore an interesting field is that of ping-pong waveforms. This is a way of implementing slow-time MIMO waveforms where one alternates between two parts of the antenna [27]. Another possible extension of this is to circulate over the antenna and transmit one pulse per antenna.

# Bibliography


[1] D. Atlas, *Radar in Meteorology*. 45 Beacon Street, Boston, MA 02176: American Meteorological Society, 1990, 10.1007/978-1-935704-15-7.

[2] A. Srivastav and S. Mandal, *Radars for Autonomous Driving: A Review of Deep Learning Methods and Challenges*. 2023. DOI: "https://doi.org/10.48550/arXiv.2306.09304".

[3] L. Liu, M. Popescu, M. Skubic, M. Rantz, T. Yardibi, and P. Cuddihy, "Automatic fall detection based on doppler radar motion signature," *5th International Conference on Pervasive Computing Technologies for Healthcare (PervasiveHealth) and Workshops*, pp. 222–225, 2011. DOI: "10.4108/icst.pervasivehealth.2011.245993".

[4] A. K. Maini, "Handbook of defence electronics and optronics: Fundamentals, technologies and systems," in first. Wiley Telecom, 2018, ch. Military Radars. DOI: "10.1002/9781119184737.ch3".

[5] J. Bergin and J. R. Guerci, *MIMO Radar Theory and Application*. Artech House, 2018.

[6] J. W. Winkler, "An investigation into ground moving target indication (GMTI) using a single-channel synthetic aperture radar (SAR)," M.S. thesis, Brigham Young University, 2013.

[7] J. Ward, "Space-time adaptive processing for airborne radar," Lincoln Laboratory, MIT, Lincoln Laboratory, MIT P.O. Box 73 Lexington, MA 02173-9108, Tech. Rep., Dec. 1994.

[8] S. T. Smith, "Wiley encyclopedia of electrical and electronics engineering," in Wiley, Dec. 1999, ch. Adaptive Radar. DOI: "10.1002/047134608X".

[9] J. Kantor and S. K. Davis. "Airborne GMTI using MIMO techniques." (2010).

[10] D. J. Rabideau, "Non-adaptive multiple-input, multiple-output radar techniques for reducing clutter," *IET Radar, Sonar & Navigation*, vol. 3, no. 4, pp. 304–313, Aug. 2009. DOI: "10.1049/iet-rsn.2008.0140".

[11] C. Kylin, T. Eriksson, A. Silander, and T. McKelvey, "Over-the-air identification of coupled nonlinear distortion in a MIMO radar," in *2022 IEEE 12th Sensor Array and Multichannel Signal Processing Workshop (SAM)*, 2022, pp. 121–125. DOI: 10.1109/SAM53842.2022.9827893.

[12] J. Li and P. Stoica, *MIMO Radar Signal Processing*. John Wiley & Sons, Inc, 2009.

[13] C. L. Weber, *Radar Detection Theory*. New York: Springer, 1987.

[14] M. A. Richards and W. L. Melvin, *Principles of Modern Radar*, second. The Institution of Engineering and Technology, Futures Place, Kings Way, Stevenag, Hertfordshire SG1 2UA, United Kingdom: SciTech Publishing, 2022, vol. 1, ISBN: 978-1-83953-381-5.

[15] Fraunhofer. "Plaque on cologne's hohenzollern bridge to commemorate the birth of radar." (Oct. 2019), [Online]. Available: `https://www.fkie.fraunhofer.de/en/press-releases/huelsmeyer_christian_plaque_cologne.html`.

[16] M. I. Skolnik, *Radar Handbook*, third. New York: The McGraw-Hill Companies, 2008.

[17] N. Mohanty, *SIGNAL PROCESSING*, first. Van Nostrand Reinhold Company Inc., 1987, DOl: 10.1007/978-94-011-7044-4.

[18] J. R. Guerci, *Space-Time Adaptive Processing for Radar*. Artech House, 2003.

[19] C. E. Shannon, "Communication in the presence of noise," *PROCEEDINGS OF THE IEEE*, vol. 86, no. 2, p. 448, Feb. 1998.

[20] P. Dammert, "On modelling for MIMO waveforms: Steering vectors in fast-time and on transmit," Oct. 2023.

[21] J. Kantor and S. K. Davis, "Airborne GMTI using MIMO techniques," in *2010 IEEE Radar Conference*, Arlington, VA, USA, May 2010, pp. 1344–1349. DOI: `10.1109/RADAR.2010.5494407`.

[22] T. McKelvey, "URA clutter modelling," Jan. 2024.

[23] T. McKelvey, "A factor representation of clutter plus noise covariance matrices," [Unpublished Manuscript], Apr. 2024.

[24] S. L. Brunton and J. N. Kutz, "Singular value decomposition (SVD)," in *Data-Driven Science and Engineering: Machine Learning, Dynamical Systems, and Control*. Cambridge University Press, 2019, pp. 3–46.

[25] J. Ward, "Space-time adaptive processing with sparse antenna arrays," in *Conference Record of Thirty-Second Asilomar Conference on Signals, Systems and Computers (Cat. No.98CH36284)*, vol. 2, 1998, 1537–1541 vol.2. DOI: `10.1109/ACSSC.1998.751584`.

[26] N. Madsen and S. Cao, "Slow-time waveform design for MIMO GMTI radar using cazac sequences," Department of Electrical and Computer Engineering, University of Arizona, IEEE, Oklahoma City, OK, USA: IEEE, Apr. 2018, pp. 1456–1460.

[27] H. Hellsten, *Meter-Wave Synthetic Aperture Radar for Concealed Object Detection*. Artech, 2017.

**DEPARTMENT OF SOME SUBJECT OR TECHNOLOGY**
**CHALMERS UNIVERSITY OF TECHNOLOGY**
Gothenburg, Sweden
www.chalmers.se


CHALMERS
UNIVERSITY OF TECHNOLOGY